3. THEORY OF THE KINETICS AND MECHANISM OF NON-CATALYTIC HETEROGENEOUS PROCESSES

3.1. Types of processes

3.1.1. Classification of processes

The classification of non-catalytic heterogeneous processes is complicated and may reflect rather different approaches[1–6]. When a homogeneous system consists of only one phase to transform, the following types of processes may be distinguished, as shown in Table 3.1. A more complicated case arises for the type: $A \rightarrow B + C$. Such a system may be limited to the case of only one solid initial phase[1–3], as given for some typical examples in Table 3.2. If the initial system is composed of two phases, containing two reacting components, the resulting processes are described by equations of the type, $A + B \rightarrow C$ and/or $A + B \rightarrow C + D$ (see Table 3.3).

This classification of heterogeneous processes, which takes into account the number and state of the phases involved, gives little information about their physical nature. A more adequate classification can be deduced from the point of view of the mechanism of the processes[1–6]. The term "mechanism" describes the path along which the process advances, i.e., the progressive succession of individual intermediate states.

TABLE 3.1

CLASSIFICATION OF PHASE TRANSFORMATIONS IN ONE COMPONENT SYSTEMS

(reactant) A		*B (product)*
(liquid)	L	G (gas)
		S (solid)
(solid)	S	G (gas)
		L (liquid)
(gas)	G	L (liquid)
		S (solid)

evaporation

sublimation

solidification

polymorphic transformation

condensation

melting

condensation

TABLE 3.2
TYPES OF SOLID-STATE REACTIONS STARTING WITH ONE SOLID PHASE

$A \rightarrow B + C$	*Type examples*
S + S	Thermal or photochemical decompositions $3AuCl \rightarrow AuCl_3 + 2Au$ $HgCl_2 \rightarrow Hg + HgCl_2$
S + L	Incongruent melting
S + G	Thermal or photochemical decompositions $CaCO_3 \rightarrow CaO + CO_2$ $2AgN_3 \rightarrow 2Ag + 3N_2$
G + G	Thermal decomposition and dissociation $NH_4Cl \rightarrow NH_3 + HCl$
G + L	Melting with decomposition

TABLE 3.3
TYPES OF SOLID-STATE REACTIONS STARTING WITH TWO SOLID PHASES

$A + B \rightarrow C$	*Type examples*
S	Alloy formation Additive powder reactions $2AgI + HgI_2 = Ag_2HgI_4$ $MgO + Al_2O_3 = MgAl_2O_4$
L	Melting of binary eutectics
G	Sublimation of binary eutectics
$A + B \rightarrow C + D$	
S + S	Substitutional powder reaction $Cu_{(s)} + AgCl_{(s)} \rightarrow CuCl_{(s)} + Ag_{(s)}$
S + G	$BaCO_{3(s)} + Fe_2O_{3(s)} \rightarrow BaFe_2O_{4(s)} + CO_{2(g)}$
S + L	Crystallization in binary system (except eutectic or peritectic compositions)

In the classification of non-catalytic heterogeneous processes from this viewpoint, two groups are generally considered:

1) Processes associated with the creation of a phase-boundary (actual formation of a heterogeneous system).

2) Processes proceeding entirely in a heterogeneous system (motion of a phase-boundary).

The heterogeneous reaction occurs on the phase-boundary and the overall process involves at least three different steps:

1) Transport of the reactants to the phase-boundary.

2) Reaction at the phase-boundary, i.e., the formation of a new phase and accomodation of atoms into the growing lattice.

3) Transport of the products away from the phase-boundary.

These principles are reflected in the more detailed scheme shown in Fig. 3.4.

In this description, only a single particle of the reacting system is considered. In the case of two reacting substances, a very fine continuous phase of a second substance surrounding the particle of the first one may be assumed and thus a similar model can be constructed.

3.1.2. Approach to the study of processes

The first step is to define the rate of the process, r. In homogeneous systems[4,5] the rate of a reaction is defined as the number of moles, n_i, of the initial substance reacting in the volume, V, per unit of time, t, or

$$r = \frac{1}{V} \times \frac{dn_i}{dt}.$$

For heterogeneous systems the rate of a process is given by the equation

$$r = \frac{1}{V_\infty} \times \frac{dV_t}{dt} \tag{3.1}$$

where V_t is the volume of the product in time t and V_∞ is the final product volume attained at the end of the reaction. The ratio

$$\alpha = V_t/V_\infty \tag{3.2}$$

is called the *fraction decomposed* (or fractional conversion or degree of reaction) and falls into the normalized range of 0 to 1. The rate of the process is a function of parameters describing the conditions of the process studied: the goal of kinetics is to find an analytical expression for it.

In general, when isothermal conditions are assumed, the kinetic equation has the form

$$d\alpha/dt = k(T) \times f(\alpha) \tag{3.3}$$

where $k(T)$ is the specific reaction rate and depends on temperature. Integrating eqn. (3.3) gives

$$\int_0^\alpha d\alpha/f(\alpha) = g(\alpha) = k'(T) \times t \tag{3.4}$$

$$d\alpha/f(\alpha) = g(\alpha) = k'(T) \times t \tag{3.4}$$

or in explicit form as

$$\alpha = k''(T) \times h(t)$$

where g and h are functions depending on the mechanism of the process.

When studying heterogeneous processes different approaches may be used. If an engineering exploitation of the process under certain conditions is the main purpose of the study, a formal description of the kinetics is sufficient. Using this formal description, $f(\alpha)$ in eqn. (3.3) has an analytical form describing the observed experimental data with a sufficient accuracy. Such an approach is usually based on a stoichiometric description of the process. The formal kinetic equation holds only for the conditions investigated and any extrapolation of it is speculative. A detailed investigation of the mechanism of the process leads to a kinetic equation that permits a broader prediction of both the rate of the process and the optimal conditions of the process realization. In this case, the function, $f(\alpha)$, in eqn. (3.3) is determined for a particular model which describes the phenomena investigated as close as possible. The selection of such a model requires a detailed investigation of the path of the process from the macroscopic down to molecular dimensions. The deduction of the mechanism and the kinetics of a process is not easy and requires a complex experimental approach.

3.2. Activated state concept

It follows from the second law of thermodynamics that every isolated system will approach an equilibrium state the properties of which are independent of time. It is required that such a reaction rate must be positive in the direction along the decrement of the system free energy and must reach a zero value at the instant of an equilibrium. However, thermodynamics is unable to say anything about the time required to attain equilibrium, the time-behavior of a system, or the configuration of a system during the period of change. A unified theory making it possible to describe processes close to their equilibrium state can be based on the thermodynamics of irreversible processes using the classical equilibrium picture as a limiting condition. However, the application of this to a relatively complex heterogeneous reactions has not been developed as yet. These problems are in the domain of chemical kinetics

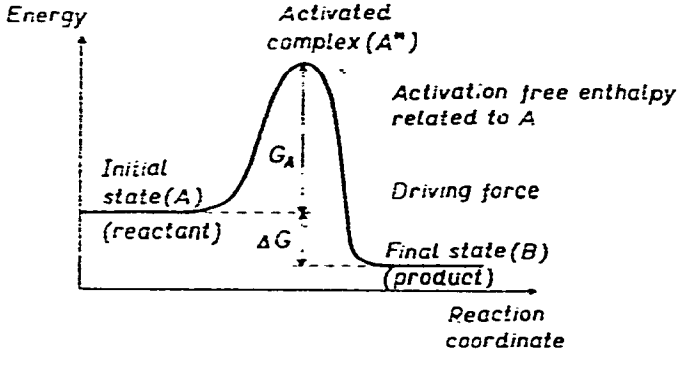

Fig. 3.1. Energetic barrier for a process.

which is directly concerned with the description of a system under transition, the properties of which are varying with time.

One of the most productive theories in modern chemical kinetics is the transition-state theory[7] which assumes that one of the intermediate states (the transition state) is a quasi-equilibrium state having a unique value of thermodynamic functions. This approach has led to establishing the unified theory of the rates of reactions based on the work of Eyring[7] and Polanyi[8]. The necessary condition for an atom (or molecule) to undergo a change is sufficient thermal energy to surmount the energy barrier which divides the initial and the final states (see Fig. 3.1). The important assumption is made as to the concentration of atoms in the activated state which are in equilibrium with the reactants. The overall reaction rate, r, is determined by the rate of the decomposition of the complexes, A^*, to the products. Mathematically, this is written as

$$r = \frac{kT}{hK^*} = kf(c) \tag{3.5}$$

where kT/h is the Boltzman constant, $f(c)$ is the function of reactant concentration and K^* is a kind of an equilibrium constant to characterize the equilibrium between the concentration of complexes and the reactants, out of the internal vibration coordinate that corresponds to passage across the barrier. On approximating $-\Delta G_A^* = RT \ln K^*$, the specific rate constant, k, in eqn. (3.5), may be expressed as

$$k = \frac{kT}{h} \exp\left(\frac{-\Delta G_A^*}{RT}\right) = \frac{kT}{h} \exp\left(\frac{\Delta S_A^*}{R}\right) \exp\left(\frac{-\Delta H_A^*}{RT}\right) \tag{3.6}$$

where ΔG_A^*, ΔS_A^* and ΔH_A^* are the free energy, entropy and enthalpy changes, respectively, associated with the activated complex formation. These quantities do not refer to the same kind of standard state for the complex as in an ordinary reaction, nevertheless, the use of these symbols has been of value in a closer understanding of the reaction kinetics.

The experimental activation energy, E (dimension: cal/mole), is defined by the relationship

$$E \equiv RT^2[\mathrm{d}(\ln k)/\mathrm{d}T] \tag{3.7}$$

The theoretical interpretation of this experimental quantity, E, can be found through the comparison of eqns. (3.6) and (3.7)

$$E = \Delta H_A^* + RT. \tag{3.8}$$

Because of a small difference between the enthalpy and energy changes in condensed systems, $E \cong \Delta U_A^* + RT$, where ΔU_A^* is the increase in the internal energy on forming the complex from the reactants.

The preexponential factor, Z (dimension: sec^{-1}), can be expressed as

$$Z = kT/h \exp(\Delta S_A^*/R) = \nu \exp(\Delta S_A^*/R) \tag{3.9}$$

where R is the gas constant and ν is the vibration frequency. It can be seen that the

reaction rate is not determined by the activation energy only. If the complex formation is accompanied by a large entropy increase the reaction rate is fast although the value retarding the activation energy may be large also. Conversely, a decrease in the activation entropy can dominate the reaction rate despite the low value of the activation energy.

A more detailed expression for the preexponential factor, Z, can be found from Zener's theory[11] of diffusivity assuming the validity of the Arrhenius-type equation

$$Z = \beta a_0^2 \Phi k \nu \exp\left[-(\Delta S_f + \Delta S_m)/R\right] \tag{3.10}$$

where a_0 is the lattice parameter, β is a geometrical constant relating a_0 to the jump distance, Φ is a constant describing the random motions of defects, $\bar{k}$ is the transmission coefficient, ν is the frequency, and ΔS_f and ΔS_m are the standard entropies of formation and motion of the diffusing defect, respectively. Many theories have been advanced in order to give a true meaning to the preexponential constant, Z[12*]. Generally, it includes many constants describing the initial state, geometry and properties of the sample. Unfortunately, such equations are usually of little value in predicting reaction rates particularly for reactions involving solids. One of the earliest attempts to treat quantitatively the rate of surface reactions, e.g., evaporation and decomposition, was by Polanyi and Wigner[8], but their results did not always agree with experimental values.

The application of statistical thermodynamics to the equilibrium constant, K^*, can be expressed in terms of the partition functions of the reactants and the activated complex and hence, the experimental reaction rate is theoretically predictable through the equation

$$k = \frac{kT}{h} K^* = \frac{kT}{h} \frac{Q^*}{Q} \exp\left(-\frac{E_0}{kT}\right) = Z \exp\left(-\frac{E_0}{kT}\right) \tag{3.11}$$

where Q^* is the complete partition function for the activated complex excluding that for the reaction coordinate; where Q is the complete partition function for the reactant, E_0 is the potential energy (i.e., energy difference between the activated complex plateau and the reactants), and Z is the frequency factor. The complete partition function can be expressed by the partial partition functions

$$Q = f^t_{\text{transl.}} f^r_{\text{rot.}} f^v_{\text{vib.}}$$

where $f_{\text{transl.}}$, $f_{\text{rot.}}$ and $f_{\text{vib.}}$ are translational, rotational and vibrational partition

*Assuming an irreversible chemical process unaffected by transfers and geometrical factors in which each quantum of absorbed energy $\Delta E (\geq N_A h\nu)$ reacted with one surfacial structural unit, Jerman (*Collect. Czech. Chem. Commun.*, 1973, in press) derived the following equations, assuming a zero-order rate constant

$$E = RT + N_A h\nu$$

$$\log Z = 15.536 + \log T + 2 \log (E/R - T) - \log M$$

where N_A is the Avogadro constant; h is the Planck constant; ν is the frequency of oscillation ($= 10^{14}\ \text{sec}^{-1}$); and M is the number of structural species ready to react at 1 m^2 of the crystal interface ($= 5 \times 10^{18}\ \text{m}^{-2}$).

functions, respectively, for the mobile groups of atoms. Mathematically, the calculation of these functions is carried out for every characteristic lattice vibration given by the degrees of freedom, t, r and r' of the molecule in the reactant and the complex. This was actually calculated by Shannon[9] for reactions of the type, $A_{solid} \rightarrow B_{solid} + C_{gas}$, and this procedure was shown in detail in the case of the first-order-like rate constant for the decomposition of $CaCO_3$. It was shown that the value of Z for this uncomplicated case is usually one or two orders of magnitude of 10^{12}. Cordes[10] also attempted to extend the above treatment for bimolecular homogeneous-like reactions; he introduced the idea that the partition function for the molecule in the solid state can be approached through the partition function for the gaseous state of the same energy (neglecting the sublimation energy), i.e., $Q_{solid} = f_{transl.} f_{rot.} Q_{gas}$. Special cases were distinguished as indicated by the different values[4] of the preexponential factors, Z (Table 3.4):

1) There is no change in degree of rotational excitation between the reactants and the complex both having completely free rotation.

2) The same as (1) but with completely restricted rotation.

3) The complex has more free conditions than the reactants which may occur on a surface where the complex extends out of the surface giving a rotation parallel to the surface (Shannon's case).

4) The reactants are assumed to have completely free rotation while that for the complex is highly restricted.

5) The reactants are in equilibrium with a surface adsorbed layer. The adsorbed species on the surface react via the activated complex to give products.

As can be seen, the empirical first-order preexponential factors may vary from

TABLE 3.4

NUMERICAL SUMMARY OF THE PREEXPONENTIAL FACTORS AT 400 K (ACCORDING TO CORDES[10])

	Preexponential factor (sec^{-1})	
	Monomolecular	*Bimolecular*
A. Bulk decomposition throughout the solid		
Case: 1	10^{15}	–
2	10^{15}	10^{16}
3	10^{16}	10^{18}
4	10^{12}	10^{10}
B. Surface decomposition (for 10 $m\mu$ particles)		
Case: 1	10^{11}	–
2	10^{11}	10^{12}
3	10^{12}	10^{14}
4	10^{8}	10^{6}
5	–	10^{6}

about 10^6 to 10^{18} sec^{-1}. The low factors would indicate a surface reaction or, if not dependent on surface area, a "tight" complex. The high factors would then mark a "loose" complex.

It is extremely difficult to theoretically predict the value of the activation energy as there is no direct correlation between the ordinary thermodynamic quantities and the height of energy barrier. Evans and Polanyi[13] attempted to give some correlations between the enthalpy change, ΔH, during a reaction and its activation energy, E. However, the real physical origin can be found in dealing with the activation energy which is connected with the diffusion mechanism. The most successful model[11] identifies E as the sum of the enthalpy to form the defect, ΔH_f, and the enthalpy for the defect to move, ΔH_m, or $E = \Delta H_f + \Delta H_m$. Diffusion mechanisms for solid-state diffusion may fall into two broad classes: rotation and defect mechanisms. It is assumed that diffusion occurs by the mechanism that has the lowest activation in the particular structure. It has been calculated in the case of copper (see Table 3.5) that

TABLE 3.5

THEORETICALLY CALCULATED E FOR THE DIFFUSION MECHANISM IN COPPER

Defect movement	ΔH_f	ΔH_m	E
Interstitial	200 (92–115)	3 (5)	203 (97–120)
2-ring rotation	–	240	240
4-ring rotation	–	90	90
Vacancy	42 (21)	23 (24)	65 (46)
Vacancy pair	37 (31)	9 (9)	40–46

Experimental = 47 kcal/mole

the vacancy mechanism is to be preferred for the lowest value of E (according to Birchenall[14]). Such considerations may be of actual help in the interpretation of activation energy values, as for example, the theoretical approach made by Pahari and Basu[15]. It is based on the idea that in the transition state certain existing bonds are breaking and at the same time certain new bonds are forming; however, it is applied to homogeneous reactions only.

In most cases, however, the investigator is referred to an experimental study of reaction rates, such as the values of activation energy and the preexponential factor, determined by means of an empirical Arrhenius-type equation. These quantities have a particular physical meaning only in the case of a known reaction mechanism, i.e., a knowledge of the model relation. In the case of a heterogeneous process, two or more steps may be involved each of them having its own specific activation barrier. For the consequent processes, where one of them has a reaction rate at least one order of magnitude lower, then this slower process serves as a rate determining impedance and becomes the rate-controlling process.

In the case of comparable rates either for consecutive or parallel processes, the overall reaction rate is a complex function of individual rate determining steps. Hence, the observed value of E indicates the mutual balance of individual processes. At any instant the value of the rate constant is the weighted mean of the individual constants. If the contribution made by the individual events changes as the transformation proceeds, the value of k varies with the progress of the transformation or with an increase in temperature. In the graphical representation of ln k vs. $(1/T)$, the most desirable plot is a straight line, as shown in Fig. 3.2. It can be seen from this

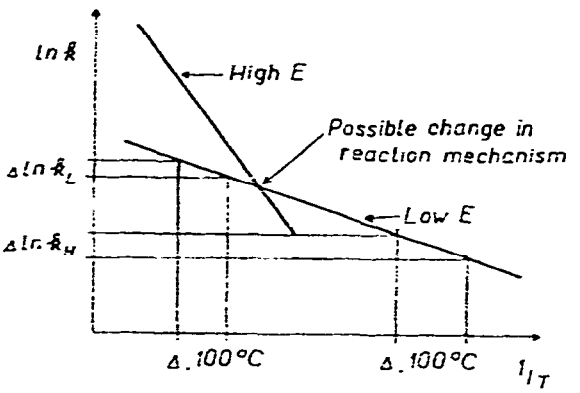

Fig. 3.2. Typical Arrhenius plot.

figure that the transition having a large activation energy is very sensitive to temperature changes and that every reaction is more sensitive to temperature changes at comparatively lower temperatures. The preexponential factor does not contribute to the reaction sensitivity with the temperature; the influence of the term, $T^m (0<m<1)$, hidden in Z, is negligible.

3.3. Homogeneous-like description of heterogeneous processes

The macroscopical approach can be used in the case where the initial system can be taken as homogeneous-like[16–18]; for example, the thermal degradation of polymers. The amount of reactants may be described in terms of the concentration (x_i) and the equations of homogeneous kinetics may be employed. In many cases, multiple simultaneous processes are likely to occur, as briefly listed in Table 3.6. The symbols, x_i, signify concentrations and/or mole fractions, the profiles of which are illustrated in Fig. 3.3. The k symbols denote the overall rate constant and the symbol, $K = k/k'$, expresses the equilibrium constant which determines the final state of a reversible reaction.

In principle, the mathematical model of such a kinetic description may be assumed to be composed of M independent equations to fit any physically complex case of j-components and i-kinetic relations, $f(x)$. It can be abbreviated as:

$$dx_j/dt = \sum_{i=1}^{N} S_{ji} k_i f(x)_{j,i} \tag{3.12}$$

TABLE 3.6

TYPES OF SIMULTANEOUS REACTIONS (see Fig. 3.3)

1. Simple reaction of n-th order	
$nA \xrightarrow{k_1} B$	$-dx_A/dt = kx_A^n$
2. Parallel reactions	
$A \xrightarrow{k_1} B$, $A \xrightarrow{k_2} C$	$-dx_A/dt = k_1 x_A + k_2 x_A$
3. Consecutive reactions	
$A \xrightarrow{k_1} B \xrightarrow{k_2} C$	$dx_B/dt = k_1 x_A - k_2 x_B = k_1 x_{A_0} \exp(-k_1 t) - k_2 x_B$
4. Autocatalytic reactions	
$A + B \xrightarrow{k_1} 2B$	$-dx_A/dt = k_1 x_A x_B = k_1 x_A (x_{A_0} - x_A)$
5. Reversible reactions	
$A \underset{k_1'}{\overset{k_1}{\rightleftharpoons}} B$	$dx_B/dt = k_1 x_A - k_1' x_B = k_1 (x_{A_0} - x_B) - k_1 x_B$

for $j = 1, 2, 3 \ldots M$ and where S_{ji} is the stoichiometric coefficient for component j. The main difficulty in the direct use of eqn. (3.12) to find the quantity, k_i, is in determining x and finding the derivatives on the left-hand side of eqn. (3.9) accurately enough; this is usually carried out by application of a non-linear least-squares regression analysis. However, eqn. (3.12) may be integrated with respect to time (assuming $S_{ji} = 1$):

$$\int_0^{x_t} dx = x(t) = \sum_{i=1}^{N} k_i \int_{t_0}^{t_h} f(x)_{j,i}\, dt = \sum_{i=1}^{N} k_i Y_{j,i,h} \tag{3.13}$$

for $h = 1, 2 \ldots, H$ (where H is the number of time intervals of x-scanning). If $x(t)$ is known and $x_{j,i}$ can be estimated, eqn. 3.13 becomes a set of linear equations for the rate constant, k_i. The system can now be solved by some discrete minimization techniques, for example, an iterative least-squares method[19,20] provided that the number of independent equations is not less than the number of rate constants. When a large number of data points are available, the integration can be accomplished by numerical quadrature[21,22] using data points. In the case of a small number of data points, one has to resort to a special curve-fitting method called split function approximation seeking a function to have continuous derivatives and stepwise continuous second derivatives[23]. Such an integrated solution to rate equations is generally used in some form to extract information from a series of measurements in terms of a homogeneous-like kinetic model. Matrix methods have been found useful for integrating the differential equations using standard computer routines or by

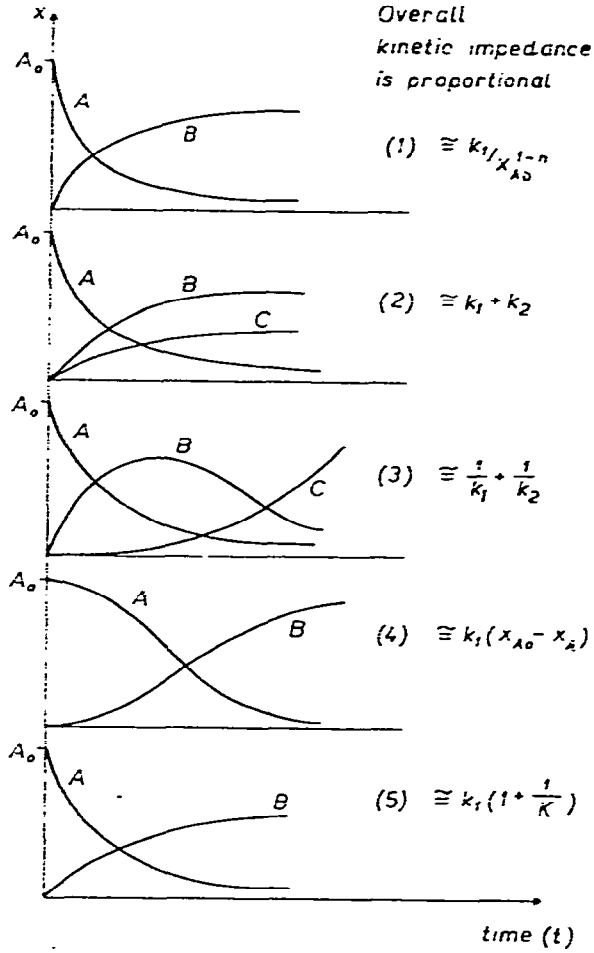

Fig. 3.3. Typical time dependences of concentration for reactants (A) and products (B, C).

means of Laplace transforms within a matrix formalism[24,25]. A similar routine has been applied to a simple composite case of the solid state reaction kinetics[26,27].

Unfortunately, the above kinetics based on reaction stoichiometry[7,8] would be a rather simplifying description of a wide variety of heterogeneous processes. The expression for the amount of reacting material in ordinary terms of concentration or mole fraction is only formal because such a quantity may vary across the sample volume. Therefore, an appropriate description should usually be based on the physico-geometrical nature of heterogeneous processes regardless of the chemical stoichiometry of reacting species.

3.4. Physico-geometrical description of heterogeneous processes

3.4.1. Choice of an appropriate model

For a description of the kinetics of phase transformation and solid state reactions numerous phenomenological theories have been proposed based upon a

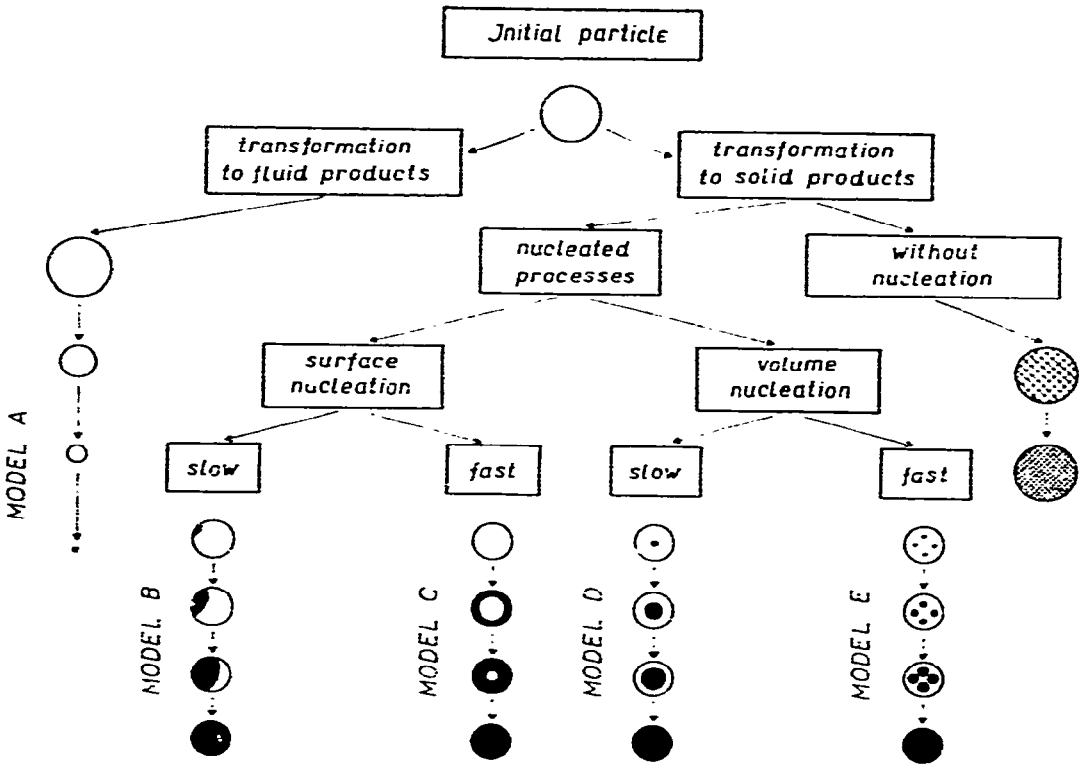

Fig. 3.4. Classification of solid-state processes.

certain model simplification[1–6,28–31]. The most important models for a single reacting particle were previously given in Fig. 3.4. The type of process must first be determined by the nature of the products; these may be: a) fluid (gaseous or liquid); or b) solid. For the first case, the process can be illustrated by model A (see Fig. 3.4), a simple shrinking particle. This is suitable in the case of sublimation, melting, and/or dissolution. Such processes proceed without nucleation or else nucleation is extremely fast and hence, negligible.

In the case of solid products and/or a mixture of solid and gaseous products, the reaction mechanism becomes more complicated. In the energetically favorable points within the unstable phase A, the stable phase B forms the product domains capable of subsequent growth until the reactant A is completely consumed. Such a transformation consists of two steps: (a) the nuclei formation; and (b) the nuclei growth. In addition, the nucleation may occur on the particle surface or throughout the particle volume. If the nucleation is slow, only a single domain on each particle is formed and the process can be illustrated by model B. If the surface nucleation is extremely fast, the reacting particle is instantaneously covered by a thin layer of the product and the rate-determining process becomes the propagation of the reacting interface into the center of the particle (model C), controlled either by diffusion or phase-boundary reactions. If the rate of surface or bulk nucleation and the rate of

nuclei growth are comparable, the overlapping of growing nuclei occurs and more complicated models are required.

For a chosen model the dependence on time of the fraction transformed can be calculated. In the case of the growth of nuclei being formed in time, $t = y$, the growth rate is given by the function $x(t)\mathrm{d}t$. The volume of all nuclei can be expressed by integration within y and t time-limits. The number of nuclei, N, presented in time, $t = y$, is determined by the nucleation rate $I = \mathrm{d}N/\mathrm{d}t$. The total amount of grown nuclei of the volume, $V(t)$, is given by the general relationship

$$V(t) = \int_0^t \left\{ \sigma \left[\int_y^t x(t)\,\mathrm{d}t \right]^{\lambda} \left(\frac{\mathrm{d}N}{\mathrm{d}t} \right)_{t=y} \right\} \mathrm{d}y \tag{3.14}$$

where σ and λ are the geometrical factor and the exponent, respectively (for a sphere $\sigma = 4/3$ and $\lambda = 3$). The procedure for determining the final model consists of the appropriate expressions for the functions, $x(t)$ and $\mathrm{d}N/\mathrm{d}t$. Combining eqns. (3.2) and (3.14), the kinetic equation for $\alpha = V(t)/V_{\infty}$ is obtained.

These models are also suitable to describe the processes in which two or more different starting phases participate: $A_{(s)} + B_{(fluid)} \rightarrow AB_{(fluid)}$, (model A); $A_{(s)} + B_{(fluid)} \rightarrow AB_{(s)}$, (model C); and $A_{(s)} + B_{(s)} \rightarrow AB_{(s)}$, (model C). It is valid under the assumption that one of the reactants is smaller than the other, acting in fact as a dispersion of larger particles in a fluid. For the last two cases above, another model has been recommended[32]; it suggests a continuous non-stationary diffusion of

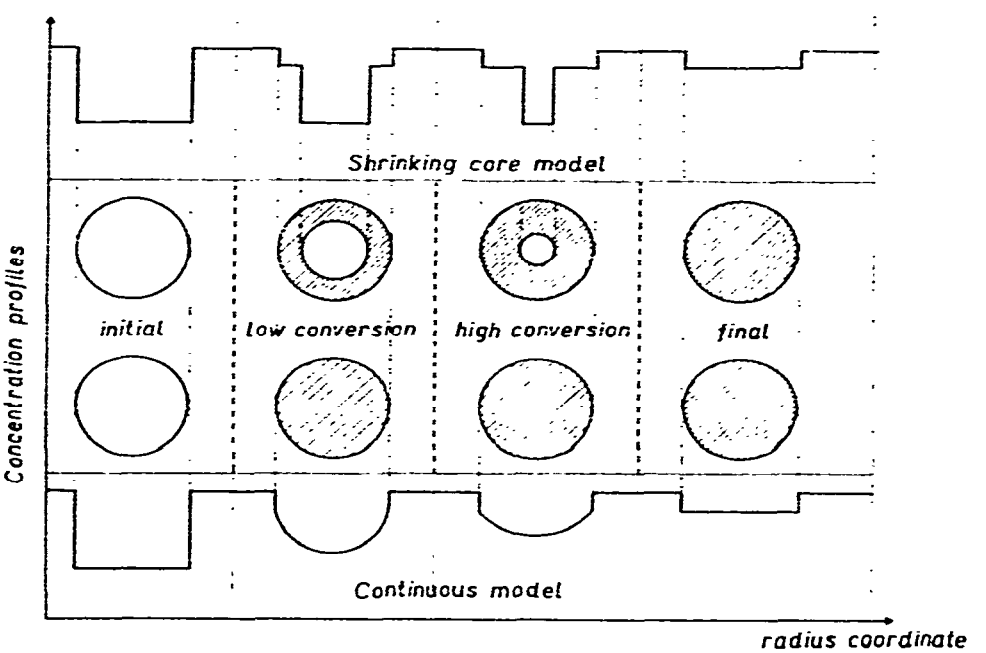

Fig. 3.5. Comparison of two different approaches for a diffusion controlled process (see model C in Fig. 3.4).

one component from the continuous-like phase into the solid particles. This model, as illustrated in Fig. 3.5, can be compared with the ordinary model of the shrinking unreacted-core particle. The macroscopic observations, however, have shown that the core-shrinking model, C, is adequate to describe most of the processes of interest.

All of the above-mentioned models assume that the initial particle is a sphere of isotropic properties with regard to the interface movement. When dealing with a single crystal this condition is not always fulfilled and for a correct description, a more complex analysis is needed. In addition, some processes in the condensed state, (ordering phenomena, martensitic transformations, spinodal decompositions) proceeds without nucleation and special models for their description are required.

The question now arises as to how far the one-particle model can be applied to a system composed of many particles. A relatively simple case, such as a monodisperse system of particles where no interaction takes place, is the decomposition of $CaCO_3$ crystals. In the case of a polydisperse system, the most logical way is to divide the original system into a series of hypothetical monodisperse sub-systems for which the above-described models are valid. The fraction decomposed is then calculated for each fraction separately and the over-all value is obtained upon their summation. In the case of two initial reacting species, the relative sizes of both particles are important. The simplest approach is for two species differing in size by at least two orders of magnitude. The larger species could then be taken as the homogeneous phase in which the particles of the second substance are suspended. The other extreme is the case of two reacting substances both monodisperse with the same particle size; such a system was treated by Komatsu (see Fig. 3.6), assuming that the reaction proceeds in contact points only.

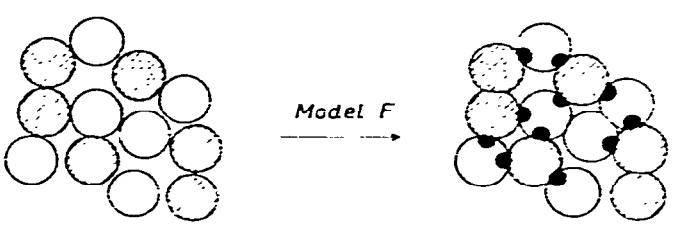

Fig. 3.6. Model for powder reactions (Komatsu model).

Until now, the driving force for a process was given by the difference of chemical potentials of the reactants and products arising from their different structure and/or chemical composition. Moreover, for a system of solid particles, the driving force may also result out of the difference between the chemical potentials assigned within the different curvature of phase boundaries. This includes sintering, i.e., the spontaneous hardening of powder compacts due to the decrease of surface energy. The sintering process may be understood as occurring in three main stages (Fig. 3.7). The beginning stage involves the initial joining of particles one to the other; the resulting kinetics obey a law derived for the growth of "necks" between the two spheres. In the intermediate stage, the pores form continuous channels along the

three grain edges. The final step of sintering involves the disappearance of isolated spherical pores. Another similar phenomenon is the growth of larger particles from the smaller ones resulting in spontaneous recrystallization of crystalline materials. The particles with negative face curvature disappear contributing to the growth of the larger particles with positive curvature, as illustrated in Fig. 3.8.

Model G

Fig. 3.7 Model for sintering process.

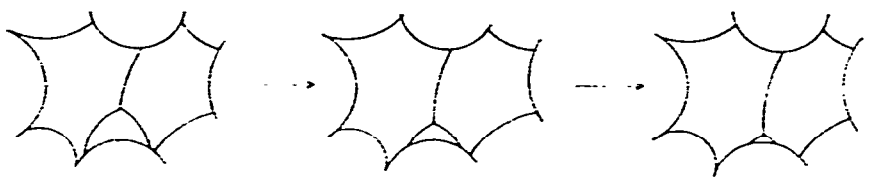

Model H

Fig. 3.8 Grain growth model.

In conclusion, it should be kept in mind that in searching for an analytical description of the reaction kinetics in solids, any function obtained is only a mathematical expression of a hypothetical model chosen to represent the process investigated. If the model actually characterizes the situation, the derived kinetic parameters will have real meaning. Otherwise, even the most elegant method of kinetic data calculation is only a mathematical exercise having little physical meaning.

3.4.2. Processes without nucleation

Transformations of the type, $A_{(s)} \rightarrow B_{(fluid)}$, proceed usually without nucleation. Such a transformation consists of two basic steps: a) a phase-boundary process; and/or b) transport processes to or from the reacting interface. The simplest cases are the evaporation of liquids, the sublimation of solids, and the dissolution of solids in liquids. A very important process is vacuum solid state sublimation, the rate of which substantially determines the lifetime of high temperature-resistant refractory materials. Langmuir[32,33] assumed that such an evaporation is accompanied by an independent condensation and at equilibrium, both of these rates become equal. The evaporating flux of molecules, r, as given per time and surface units, can be expressed under steady state conditions by

$$r = \frac{P_{eq}}{(2\pi MRT)^{1/2}} \tag{3.15}$$

As derived from kinetic theory by Hertz[32,33], P_{eq} is the equilibrium partial pressure

of the gaseous product of molecular weight M. According to Langmuir[32,33], this pressure, P_{eq}, remains unchanged even in the case of sublimation into vacuum

$$P_{eq} = \exp(-\Delta G_v^\circ/RT) \tag{3.16}$$

where ΔG_V° is the standard change of the Gibbs free energy of sublimation. Combination with eqn. (3.15) gives

$$r = (2\pi MRT)^{1/2} \exp(-\Delta G_v^\circ/RT) \tag{3.17}$$

Knudsen[32,33] has shown that the right-hand side of eqn. (3.17) must be multiplied by a coefficient, α', which represents the fraction of gaseous molecules reaching equilibrium upon their collisions with the condensed phase ($\alpha' = 1$ when all molecules undergo the condensation upon their contact against the surface). This means that the sublimation kinetics is described by a two step mechanism consisting of the surface reaction and the desorption[32,33]. For the evaporation of pure liquids under atmospheric pressure, a rapid change of the phase-boundary is assumed and the rate-controlling process becomes the diffusion through the surface gas layer. The solution for the different cases can be found in the work of Crank[34] or in the monograph on transport phenomena[35].

Similarly, one can proceed to binary liquid solutions where the rate controlling process is also diffusion, but in the liquid phase along the direction perpendicular to the phase-boundary. Hence, the dissolution of a solid in a liquid is determined by either a simple dissolution or a chemical reaction (dissolution of $CaCO_3$ in HCl). It consists of a two-step mechanism: a) the process on the phase-boundary, and b) mass transport. In the simple case of a dissolving solid, the rate is described by the rate of surface reaction expressed by the consumption of solid, m, per unit time:

$$-dm/dt = kA(C^\circ - C) \tag{3.18}$$

where A is the surface of the phase boundary, and C and C° are the bulk and saturated concentrations of the solute.

Equation (3.18) is first order with regard to the solute. If the surface reaction is faster than the mass transport, the diffusion becomes the rate determining process. Under steady-state conditions the diffusion takes place through a liquid layer adhering on the solid surface and having the effective thickness, δ_{eff}. The rate of dissolution is then

$$-dm/dt = (D/\delta_{eff})A(C^\circ - C) \tag{3.19}$$

where D is the diffusion coefficient and δ_{eff} can be theoretically calculated for the particular hydrodynamic conditions. In general, the following equation is valid

$$-\frac{dm}{dt} = \frac{kA(C^\circ - C)}{\left(\frac{1 + k\delta_{eff}}{D}\right)} \tag{3.20}$$

where $k \ll D/\delta_{eff}$ in eqn. (3.18), and $k \gg (D/\delta_{eff})$ in eqn. (3.19); the concentration profiles for both of these cases are shown in Fig. 3.9.

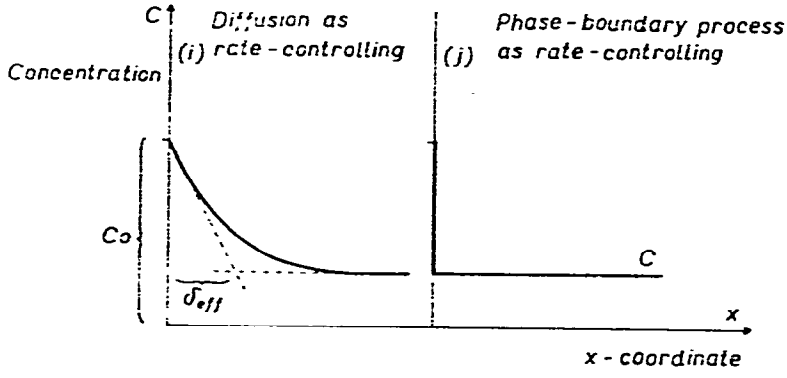

Fig. 3.9. Concentration profiles at solid–liquid interface.

In considering a dissolving solid particle, its surface becomes a function of time, $A = A(t)$. Assuming that the particle shape remains constant during its dissolution, then $A = km^{2/3}$, where m is the particle mass. If the particle of initial mass, m^*, is being dissolved in a liquid of volume V, then the amount dissolved in time t is given by $m^* - m$, and the rate of dissolution by an equation described by Hixson and Crowel[36,37]:

$$\frac{dm}{dt} = \frac{k}{V}(m_0 - m^* + m)\, m^{2/3} \tag{3.21}$$

where m_0 is the amount of solid material to form the saturated solution ($C_s = m_0/V$). Assuming that for $t = 0$, the concentration, $C = (m^* - m)/V = 0$, integration of eqn. (3.21) yields

$$\frac{V}{a^2}\left(\sqrt{3}\,\text{arct}\,g^2\,\frac{\sqrt{3}\,a(b-x)}{3a^2+(2b-a)(2x-a)} + 1.15\ln\frac{(a+b)(a^2-ax+x^2)}{(a+x)(a^2-ab+b^2)}\right) = kt \tag{3.22}$$

where $a = m_0 - m^*$, $b = m^{*1/3}$ and $x = m^{1/3} = (CV)^{1/3}$. In the case of unsteady diffusion (dissolution in viscous fluids), the rate of particle dissolution was derived by Readey and Cooper[38]

$$\frac{\partial c^*}{\partial x^*} = \frac{\partial^2 c^*}{\partial r^{*2}} + \frac{2}{r^*}\frac{\partial c^*}{\partial r^*} + \frac{a^{*2}}{r^{*2}}(A-1)\frac{da^*}{dt^*}\frac{\partial c^*}{\partial r^*} \tag{3.23}$$

$$\frac{da^*}{dt^*} = B\left(\frac{\partial c^*}{\partial r^*}\right)$$

where

$$a^* = \frac{a}{a_0},\quad r^* = \frac{r}{a_0},\quad c^* = \frac{C - C_\infty}{C_s - C_\infty},\quad t^* = \frac{Dt}{a_0^2}$$

are dimensionless parameters and

$$B = \frac{(C_a - C_x)}{(C_s - C_a C_s \bar{V})} \quad \text{and} \quad A = \overline{VC_s}$$

The symbols are C_x = initial concentration of the solute, C_a = saturation concentration at the phase boundary, a = sphere radius, t = time, r = radial distance, C_s = density of the solid (sphere), D = diffusivity and V = partial specific volume of the solute. In the case of a surface process of n-th order being the rate-determining step, the rate of dissolution related to the concentration of the solute is given by the equation of Stavrinou and Blumberg[39].

3.4.3. Nucleation-dependent processes

This type of transformation includes all polymorphic transitions and dissociation reactions of solids, as illustrated by models B, C, D, E in Fig. 3.4.

3.4.3.1. Nucleation. The rate of nucleation, I, is defined as the number of stable product domains formed within a unit time interval in a unit volume of the matrix. As long as the nuclei are created purely randomly throughout the whole reactant volume, the process is called homogeneous nucleation. If the nucleation proceeds on foreign, energetically preferred areas (walls of a reacting chamber, particles of impurities or even dislocations) then it is called heterogeneous nucleation.

The classical theory of nucleation in a one component, single-phase system indicates that the temperature activated fluctuations of atoms (or molecules), which gather into a certain critical size capable of a spontaneous growth, is accompanied by a decrease of the Gibbs free energy of the system. Such product clusters are designated as nuclei and their size is given by the thermodynamic criterion of stability. The change of free energy coupled with the creation of an embryo of phase B within the surrounding medium of the phase A is given by

$$\Delta G = i(G_v + \sigma)\lambda + \beta i^{2/3}\gamma \tag{3.25}$$

where i is the number of atoms in the embryo, λ is the atomic volume, β is the embryo shape factor, σ is the energy increment resulting from the elastic strain which is associated with volume changes during the transformation, γ is the interface energy, and ΔG_v is the difference in the Gibbs free energy of the bulk phases A and B per unit volume. In the case that one of the phases is a liquid, the quantity σ can be neglected. Assuming a spherical shape of the embryo, the function, ΔG, reaches a maximum for nuclei of the radius, r_{crit}

$$r_{crit} = -2\gamma/\Delta G_v. \tag{3.26}$$

The energy height, W (maximum value of ΔG) is

$$W = (16/3)\,\pi\gamma^3/\Delta G_v^2. \tag{3.27}$$

The quantity, ΔG_v, may be approached by the relationship, $\Delta G_v = RT \ln (P/P_e)/V_m^2$.

for the condensation from a vapor or by $\Delta G_v = H_v(T - T_e)/T_e$, for the crystallization or melting at small departures from equilibrium (where P and P_e are the actual and equilibrium vapor pressure, V_m is the molar volume, ΔH_v is the heat of fusion per unit volume and T and T_e are the actual and equilibrium temperatures respectively).

Volmer and Weber[40] assumed that for the rate of nucleation the concentration of critical nuclei is a characteristic of equilibrium. Hence, the rate of nucleation per unit volume is a product of the equilibrium number of embryos of critical size per unit volume and the rate of interface movement. Combining the absolute reaction rate theory with the Volmer and Weber approach, Becker and Döring[41] have derived the relationship,

$$I = Z \exp(-E_D/kT) \exp(-W/kT) \tag{3.28}$$

where E_D is the activation energy for motion across the embryo–matrix interface and Z is the frequency factor which may be taken to an order-of-magnitude accuracy as $Z = N_v^0 \times \nu_0$. The quantity, N_v^0, is the number of unassociated molecules per unit volume and ν_0 is the molecular jump frequency. From eqn. (3.28) it follows that at the equilibrium temperature, T_{eq}, $I = 0$, because of $\exp(-W/kT) = 0$ (see eqn. (3.27)). The function I has a maximum on account of the competitively opposite influence of the terms, $\exp(-W/kT)$, which increases its value with decreasing temperature, and $\exp(-E_D/kT)$, which decreases its value to zero ($E_D \simeq$ constant).

In the case that both phases A and B are solids, the quantity, σ, in eqn. (3.25) influences the shape and the size of the nuclei. Two types of such nucleation processes are usually assumed:

(1) *Incoherent nucleation*, where the nucleus and the host matrix do not have a crystallographic continuity (where $\gamma \cong 200$–1000 erg/cm^2 has the essential weight in the value W, see eqn. (3.27)), and

(2) *Coherent nucleation*, where both of the phases remain in surface contact with the crystallographic structure which is very similar, e.g., the atomic distances in the surface are almost identical. The term, γ, is small and the nuclei shape is determined by the elastic constants of both phases. Such nuclei are oriented in a certain crystallographic direction with regard to the original phase A.

In a multicomponent homogeneous system, the variable quantities are both the nuclei size and the nuclei composition. The classical theory of homogeneous nucleation was extended for binary systems by Becker[42]. In this approach, the first step is to calculate the embryo composition in connection with the required decrease of the system free energy ($\Delta G_v < 0$). For the sake of simplicity, the immiscibility type of a binary phase diagram is shown in Fig. 3.10. The homogeneous material of a chosen composition, X_B, is cooled down to a region of temperature where the equilibrium configuration consists of the phase A (composition, X^α) and the phase B (composition, X^β). The equilibrium composition is given by the contact points of the free energy curve with the common tangent. The change in the free energy on forming clusters of composition X^β is given by the difference ΔG_v, see Fig. 3.10 (refs. 45–47).

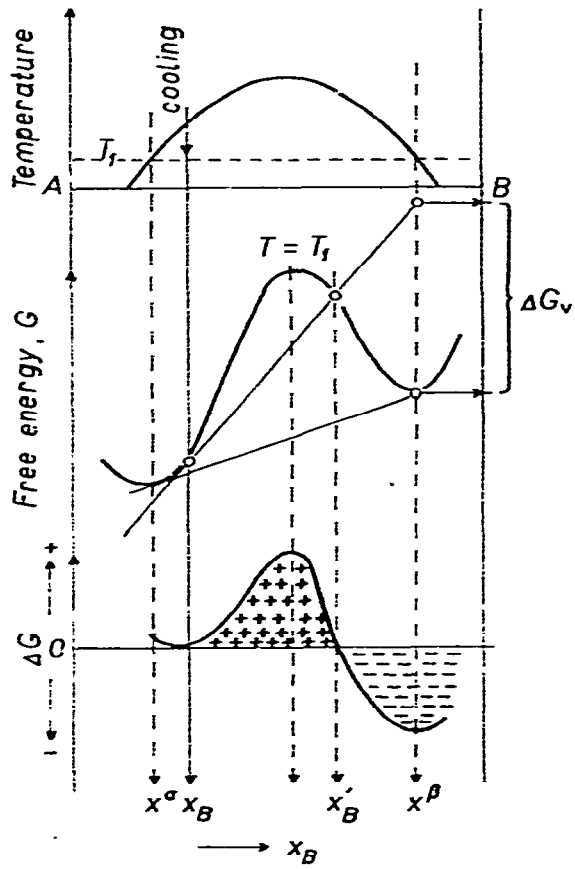

Fig. 3.10. Binary system with limited miscibility (see text). a) miscibility gap (phase diagram); b) graphical determination of free energy change associated with nucleus formation; c) free energy change connected with new phase formation as a function of its composition.

For the system depicted in Fig. 3.10, the initial homogeneous system, X_B, is stable with respect to the formation of clusters with a composition between X_B and X'_B (increase in the volume free energy). The clusters of the composition on the right-hand side of X'_B are unstable with respect to the formation of X^β, and the previous formalism of eqns. 3.26 and 3.27 may be used. The created cluster must fulfil the condition for minimum W (eqn. 3.27), which is determined by the balance between ΔG_v and γ. For simpler cases, Becker assumed that the nucleus holds the composition of the stable phase B and its size is given by the surface energy γ. On the other hand, Borelius[43] neglected the influence of γ (= constant) using the decisive influence of fluctuation in the composition. In practice, the critical nucleus characterized by the least work of formation for the given conditions reflects the balance of these two influences. The nature of such a critical nucleus was introduced by Hobstetter[44] and more precisely by Cahn and Hilliard[45]. The latter found that at low supersaturations, the nucleus has the composition of the stable phase forming a sharp interface. With increasing supersaturation, the interface between the nucleus and the

host matrix becomes progressively more diffuse and the embryo composition is a function of the distance from its center. When the inflection point on the free energy curve is approached, the work of critical nucleus formation decreases to zero. Thus, in the vicinity of the so-called spinodal, the critical nucleus no longer resembles a cluster of the new phase, but rather represents a fluctuation small in degree but large in its extent in space. It can best be illustrated on Fig. 3.11 where the initial com-

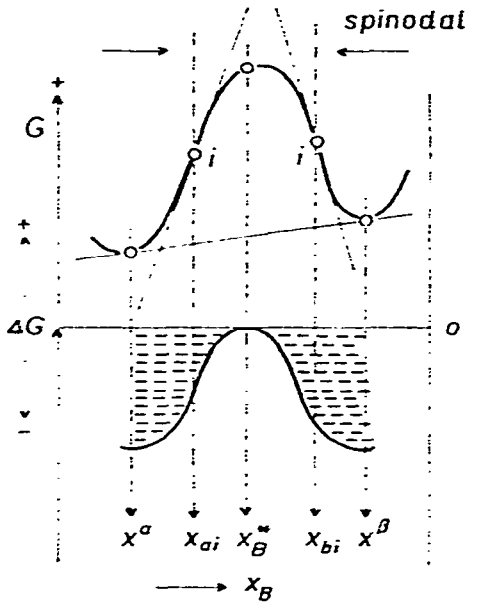

Fig. 3.11. Condition for spinodal decomposition (see text).

position X_B falls within the region limited by the inflection points, X_{ai} and X_{bi}. The free energy decreases along with the continuous change in the composition of both precipitated phases. Such a process is called *spinodal decomposition*[4-6].

The theory of heterogeneous nucleation is based on the determination of the quantity, W (eqn. 3.27). In order to initiate the nucleation the impurity interfaces may decrease the nucleation barrier W according to:

$$W = \frac{16}{3}\pi\frac{\gamma^3}{(\Delta G_v)^2}\left[\frac{(2+\cos\theta)(1-\cos\theta)^2}{4}\right] \tag{3.29}$$

where θ is the contact angle of the three-phase boundary (domain of phase B, matrix A and impurity surface). For nucleation in solids, the quantity W is decreased by either the decrease in the quantity γ (or σ) or by an increase in the negative value of ΔG_v. It is assumed that most of the potential embryos are already present in solids and the entire nucleation process demands only that their development become stable. Thus, if N_0 is the number of such potential embryos in a volume element of a solid, the nucleation rate can generally be expressed by the relationship,

$$I = dN/dt = k_1(N_0 - N)^s \tag{3.30}$$

which is called the power law. The exponent, β, expresses the number of activated steps and is usually equal to one. The nucleation rate can also be described by the exponential law,

$$I = k_1 N_0 \exp(-k_1 t) \tag{3.31}$$

If the rate constant, k_1, is small the number of nuclei is given by

$$N \cong k_1 N_0 t \tag{3.32}$$

but if k_1 is large, the nucleation is extremely fast so that the nuclei are formed instantaneously on all of the available nucleation spots, yielding $N \cong N_0$.

3.4.3.2. Growth of the precipitated phase. The growth of a nuclei is signified by the motion of a phase boundary in the direction of the unstable phase, A. In solids this process can be controlled by either the mass transport (diffusion controlled transformation) or by the shear of large areas in the initial phase lattice yielding new crystallographic arrangements (phase-boundary reaction). In a single component system[47], the linear rate of the propagation of phase-boundary can be expressed as the velocity difference with which the atoms (or molecules) overcome the energy barrier on the interface matrix–embryo

$$r = \lambda p N_s \nu \left[A_B \exp\left(-\frac{E^{A\to B}}{RT}\right) - A_A \exp\left(-\frac{E^{B\to A}}{RT}\right)\right] \tag{3.33}$$

where λ is the atomic volume of the phase B, p is the probability of jumping of an atom along the positive transport direction, and ν is the vibration frequency in phase A. The terms, A_A and A_B, are the accommodation coefficients in phase A and B, respectively; N_s is the number of atoms per unit area of the phases interface, and E is the activation energy for the given barrier crossing (A → B and B → A, resp.). Assuming that for polymorphic transformations, $A_A \cong A_B \cong A$, eqn. (3.33) can be rearranged to[47]

$$r = \lambda p N_s \nu A \left[\exp\left(-\frac{E^{A\to B}}{RT}\right)\left(1 - \exp\left(\frac{\Delta G}{RT}\right)\right)\right]. \tag{3.34}$$

For a small degree of supersaturation, $T = T - T_c$, eqn. (3.34) may be rewritten as

$$r = \lambda N_s A D^* \left(\frac{\Delta G}{RT}\right) \Delta T \tag{3.35}$$

where D^* is the diffusion coefficient for the diffusion along the grain interfaces.

For a multicomponent system, the rate of growth at which the product–parent interface moves normal to itself may be controlled either by an interface (topochemical) process or a diffusional transport or their combination. In principle, the analogous relations are valid as derived for model A.

3.4.3.3. Nuclei growth as the rate determining step

(*a*) *Phase-boundary controlled growth.* Using eqn. (3.13), it is possible to calculate the

volume of the product, $V(t)$, and the dependence of the function $f(\alpha)$ on time t, for the given model of the process.

Models B, D and E. For the normal type of random nucleation (exponential law, rate constant k_1) and the isotropic linear growth rate in three dimensions (rate constant k_2), the classical solution of eqn. (3.13) gives[48]

$$\alpha = \frac{8\pi N_0 k_2^3}{V_0 k_1^3}\left[\exp(-k_1 t) - 1 + k_1 t - \frac{(k_1 t)^2}{2!} + \frac{(k_1 t)^3}{3!}\right]. \tag{3.36}$$

If N_0 is large and k_1 is small, indicating a constant rate of nucleation (linear law eqn. (3.32)), the exponent term can be extended in a series. Neglecting greater terms than $(k_1 t^4)$, eqn. (3.36) gives

$$\alpha = \frac{\pi N_0 k_2^3 k_1}{3 V_0} t^4 \tag{3.37}$$

A similar relation, α vs. t^4, was also derived by Mampel[49] for the initial stages of a decomposition reaction. At the other extreme, if k_1 is very large (instantaneous nucleation, eqn. (3.32)), the term with the highest exponent has the predominant influence so that all of the other terms can be neglected and eqn. (3.36) yields

$$\alpha = \frac{4\pi N_0 k_2^3}{3 V_0} t^3 \tag{3.38}$$

and the corresponding rate by

$$\frac{d\alpha}{dt} = \frac{4\pi N_0 k_2^3}{V_0} t^2 \tag{3.39}$$

However, certain nucleus forming sites will never allow nuclei to grow because these sites become incorporated in other growing nuclei before their activation. The effective interfacial area is then introduced as $(1-\alpha)$ in the right-hand side of eqn. (3.39) (Yerofeyev[50]); after integration,

$$\alpha = 1 - \exp\left[\frac{-4\pi N_0 k_2^3}{3 V_0} t^3\right]. \tag{3.40}$$

The problem of accounting for the fact that the fraction transformed when nuclei overlap one another is less than the value of α calculated on basis of eqns. (3.36)–(3.38) may be solved in a quite general way by introducing the concept of extended fractional transformation, α_{ex}, using the equation

$$d\alpha = (1-\alpha)\, d\alpha_{ex} \text{ and/or } \alpha_{ex} = \int_0^{\alpha} d\alpha/(1-\alpha) = -\ln(1-\alpha) \tag{3.41}$$

The term, α_{ex}, is the fraction transformed if all of the domains had grown without interpenetration and nuclei had continued to form everywhere in the sample including the already transformed volume. The resulting eqn. (3.41) may then be introduced

back into eqn. (3.36)[48].

A more instructive method of kinetic analyses[52–54] is based on the following assumptions (see eqn. 3.13): the volume of domains ready to grow is $k_2^3(t-y)^3$ at time y and for the specific rate constant of omnidirectional growth k_2; the rate of nucleation per unit volume is I and the total number of nuclei formed is $I\mathrm{d}y$. For three-dimensional symmetry

$$\alpha_{ex} = \frac{4}{3}\pi k_2^3 \int_0^t (t-y)^3 I \,\mathrm{d}y. \tag{3.42}$$

Using α_{ex} from eqn. (3.41) and making an assumption about the variation of I with time in accordance with section 3.4.2, eqn. (3.42) can be integrated. For a constant nucleation rate, k_1,

$$-\ln(1-\alpha) = (\pi/3)\, k_2^3 k_1 t^4. \tag{3.43}$$

If all nuclei are already present at time $y = 0$ (initial number N_0) eqn. (3.43) changes to

$$-\ln(1-\alpha) = \tfrac{4}{3}\pi N_0 k_2^3 t^3 \tag{3.44}$$

In the case of only two-dimensional growth, eqn. (3.44) changes to

$$-\ln(1-\alpha) = N_0 \pi h k_2^2 t^2 \tag{3.45}$$

where h is the disk-like nuclei thickness.

In highly dispersed systems where random nucleation forms only a single nucleus in an individual particle (see model B—Fig. 3.4), the kinetics is then described by a unimolecular decay law

$$-\ln(1-\alpha) = k' t \tag{3.46}$$

derived by Mampel[49] for final stages of decompositions. In most of these cases, the resulting equation can be abbreviated in the formal form of the Johanson–Mehl–Avrami–Yerofeyev–Koglomorov relation[49–53,108]

$$-\ln(1-\alpha) = kt^r = Z \exp(-E/RT)\, t^r. \tag{3.47}$$

The value of the exponent, r, depends on the shape of product domains, on the rate of nucleation, and the type of subsequent growth-controlling process, as listed[54,109] in Table 3.7. The complex activation energy, E, is composed of the activation energies of the individual process[55], i.e., of nucleation, E_1, growth, E_2 and diffusion, E_D. The quantities, E_1 and E_2, are further composed of two terms: the first arising from the kinetic barrier to transport and the second from the thermodynamic work barrier dependent on the extent of supercooling, as discussed in section 3.3.1 (eqn. 3.27). The preexponential factor, Z, depends predominantly on the geometry and number of nuclei to be formed.

In some cases the formation of additional nuclei, as considered for example in linear nuclei growth, is a more important process than the formation of fresh nuclei

TABLE 3.7

NUMERICAL VALUES FOR THE KINETIC EQUATIONS OF NUCLEATION AND CRYSTAL GROWTH: $-\ln(1-\alpha) = Z\exp(-E/RT)t^r$

For the increasing rate of nucleation the exponent r is larger than that for the constant nucleation rate. For the decreasing rate of nucleation the exponent r falls between that of the constant and that of the zero nucleation rates.

		Phase-boundary controlled: $x(t) = k_2 t$		*Diffusion controlled:* $x(t) = (Dt)^{1/2}$	
		r	E	r	E
Constant rate of nucleation: $I = k_1 t$	spheres	4	$3E_2 + E_1$	2.5	$\frac{3}{2}E_D + E_1$
	plates	3	$2E_2 + E_1$	2	$E_D + E_1$
	needles	2	$E_2 + E_1$	1.5	$\frac{1}{2}E_D + E_1$
Zero rate of nucleation: $I = N_0$	spheres	3	$3E_2$	1.5	$\frac{3}{2}E_D$
	plates	2	$2E_2$	1	E_D
	needles	1	E_2	0.5	$\frac{1}{2}E_D$

and the initial nucleation law is relatively less important. Assuming the branching coefficient k_3, the net rate of nuclei production is given by

$$dN/dt = k_1 N_0 + k_3 N \quad \text{and/or} \quad N = k_1 N_0/k_3[\exp(k_3 t) - 1] \tag{3.48}$$

which is suitable to describe some explosive reactions. Using a similar procedure to eqns. (3.12) and (3.36), the fraction decomposed, α, is

$$\alpha = Fk_1 k_2 N_0/V_0 k_3^2 \exp(-k_3 t) \tag{3.49}$$

where F is the cross-section of the nucleus.

Prout and Tompkins[56] solved the case of interfering branching nuclei growth by introducing the probability of termination, $k_\perp = k_3\alpha/\alpha_i$; where α_i is the fraction decomposed at the inflection point. The final equation is then

$$d\alpha/dt = k_3\alpha(1-\alpha) \quad \text{and/or} \quad \ln[\alpha/(1-\alpha)] = k_3 t + \text{constant} \tag{3.50}$$

which is the simplest case of the description of an autocatalytic reaction where the reaction velocity is a function of both the amount of the reactant and the product[82,83].

(*b*) *Diffusion-controlled growth.* The transition of melts to the solid state upon their cooling may proceed either by crystallization or by the formation of a glass[57]. Which of these two processes actually takes place is determined by the rate of cooling and by the differences in temperature profiles of the rate of nucleation and the rate of crystal growth. In Fig. 3.12, two characteristic cases are shown.

System A will solidify by crystallization regardless of the rate of cooling because there is always enough nuclei formed to grow at a lower temperature[58]; on

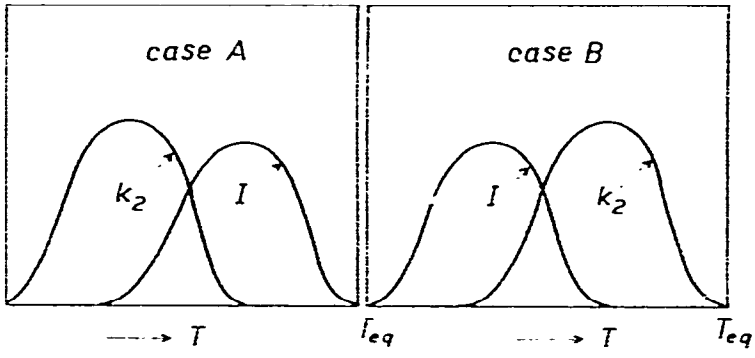

Fig. 3.12. Temperature dependence of nucleation (I) and crystal growth (k_2) rates for two typical cases.

the other hand, system B will easily form a glass, particularly at high rates of cooling because in the region where the rate of nucleation is large, the rate of growth is already negligible. Actual systems exist somewhere in between these two extreme cases.

For case A, there are numerous models suggested for the crystallization from both pure melts and solid state solutions. To describe reaction kinetics of the exponential type, the Johanson–Mehl–Avrami–Yerofeyev–Koglomorov equation is derived usually on behalf of diffusion controlled growth (latter stages of crystallizations). For example, the kinetics of a single phase crystallization in a two component system can be assumed. The rate of growth depends upon the rate at which atoms are brought to the interface through the melt. The concentration in the solution at the interface is maintained at the equilibrium value C_E, which is independent of precipitate size and C_β is the actual solute concentration. The concentration of the solution decreases as precipitation progresses and can be expressed in terms of α, the fraction of the available solute actually precipitated at time t, or

$$1-\alpha = (C_{(t)}-C_E)/(C_I-C_E) \tag{3.51}$$

where C_I and $C_{(t)}$ are initial and instantaneous concentrations in the solution.

The diffusional rate of growth is given[47,59,60] by

$$(C_\beta - C_E)\, dR/dt = D(\partial c/\partial r)_{r=R} \tag{3.52}$$

where R is the radius of the particle. Using the steady state solution of Fick's equation for diffusion through a spherical shell, with diffusion coefficient D independent of C and replacing $C_{(t)}$ by α through eqn. (3.51), the expression is obtained:

$$R\frac{dR}{dt} = D\frac{C_I - C_E}{C_\beta - C_E}(1-\alpha) \tag{3.53}$$

Assuming growth without nucleation, i.e., diffusion-controlled growth of a fixed

number of particles N_0, the following equation is derived[61,62]

$$\alpha = 1 - \exp\left[-\frac{8}{3} \sqrt{2}\, \pi N_0 D^{3/2} \left(\frac{C_I - C_E}{C_\beta - C_E} \right)^{1/2} t^{3/2} \right]. \tag{3.54}$$

Or using the assumption that the constant rate of nucleation I changes by the exponent of time to 5/2,

$$\alpha = 1 - \exp\left[-\frac{16}{15} \sqrt{2}\, \pi D^{3/2} \left(\frac{C_I - C_E}{C_\beta - C_E} \right)^{1/2} k_1 t^{5/2} \right]. \tag{3.55}$$

The exponent of time, r, changes according to the mathematical solution of the equation; for instance, in diffusion-controlled growth of cylindrical particles, $r = 1$; for disklike particles, $r = 2/3$; and or eutectoidal crystallizations, $r = 3$ and 4; these are summarized in Table 3.7. Similar relations can be employed to describe precipitation from aqueous solutions[60,63].

Model C. This type of process includes reactions between solids and gases, solids and liquids and in some special cases, solid–solid reactions (if one reactant is assumed as a continuous medium). Such reactions can be described by model C, Fig. 3.4, when the rate determining process may become either diffusion through the product layer or phase-boundary reaction.

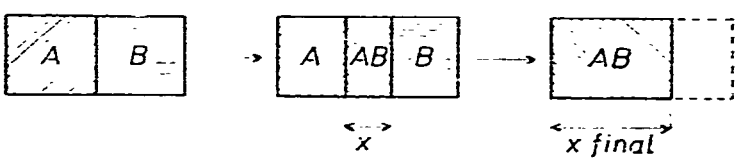

Fig. 3.13. Model of a reaction between two solids.

3.4.3.4. Processes proceeding by instantaneous surface nucleation

(*a*) *Diffusion-controlled reactions.* If one of the components participating in the reaction must penetrate through the layer dividing two reacting phases A and B (see Fig. 3.13), the time dependence of gradual build up of this planar product layer can be described by the parabolic law

$$x^2 = 2DV_m C_0 t + a^{1/2} \tag{3.56}$$

where x is the thickness of the product layer, D is the diffusion coefficient for the slowest transport (vacancies, interstices, etc.), V_m is the volume of product AB formed from 1 mole of the lowest penetrating component, C_0 is the concentration of the penetrating component on the interface and a is the layer thickness at time $t = 0$. Jander[110] applied the parabolic rate law to powdered compacts (see Fig. 3.14) which, expressed as a function of fractional transformation, α, can be written as

$$[1 - (1-\alpha)^{1/3}]^2 = 2kD/r_0^2 \times t. \tag{3.57}$$

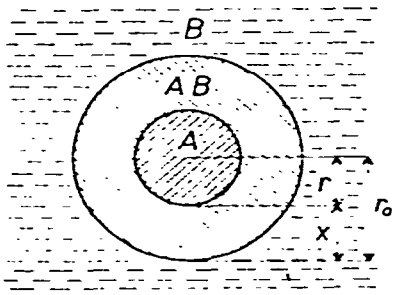

Fig. 3.14. Model for a powder reaction (Jander).

This equation is valid under certain simplifying assumptions[110], namely, that of the instantaneous surface nucleation (coherent product layer is already present when bulk diffusion does occur), an omni-directional bulk diffusion, and the immiscibility of the product phase with any of the reactant phases. It is further assumed that the reacting particles are spheres of uniform radii and that the diffusion coefficient and reactant activity as well as the particle volume are constant during the process.

Kroger and Ziegler[59] assumed that the diffusion coefficient of the transported species was inversely proportional to time,

$$[1-(1-\alpha)^{1/3}]^2 = 2k/r_0^2 \times \ln t. \tag{3.58}$$

Zhuravlev, Lesokhin and Tempelman[111] modified the Jander relation by assuming that the activity of the reacting substance was proportional to the fraction of unreacted material, $(1-\alpha)$, and arrived at the expression

$$\left[\frac{1}{(1-\alpha)^{1/3}} - 1\right]^2 = \frac{2kD}{r_0^2} t \tag{3.59}$$

Ginsling and Brounshtein[113] discarded the parabolic law in favor of an equation relating the growth of the product layer to the decrease in interface area using Barrer's equation[112] for steady-state heat transfer across a spherical shell, and obtained the equation

$$1 - \frac{2}{3}\alpha - (1-\alpha)^{2/3} = \frac{2kD}{r_0^2} t. \tag{3.60}$$

Carter[64] and Valensi[65] improved eqn. (3.58) by accounting for differences in the volume of the product layer with respect to the volume of the reactant consumed,

$$Z-(Z-1)(1-\alpha)^{2/3} - [1+(Z-1)\alpha]^{2/3} = \frac{2kD(Z-1)}{r_0^2} t \tag{3.61}$$

where Z is the ratio of the actual volume of the product layer to the ideal volume if no change occurs. Huibert[54] used the assumptions of eqn. (3.56) and replaced t by $\ln t$ in eqn. (3.61). Such an equation adequately describes the probability of removal of the non-equilibrium defect state and has an exponential dependence on temperature.

Komatsu and Uemura[66] introduced counter-diffusion arriving at an "anti-Jander" equation

$$[(1+\alpha)^{1/3}-1]^2 = \frac{2kD}{r_0^2}t \tag{3.62}$$

All of the above equations express the unreacted-core-shrinking model which, in most cases, adequately describes the real situation. For some reactions it is more convenient to introduce an idea of a continuous reaction (as already illustrated in Fig. 3.5) where reactant B is bulk adsorbed by the reactant-particle A, the whole volume of which is continuously changed to product AB. Dünnwald and Wagner[67] and Serrin and Erlickson[68] used this model to describe the kinetics in powder systems. The fractional conversion, α, given by the ratio of the mole number of component B adsorbed into particles A in time t per mole of B finally adsorbed when the reaction is completed, is equal to

$$\alpha = 1 - \frac{6}{\pi^2}\sum_{n=1}^{n=\infty}\frac{1}{n^2}\exp(-n^2kt) \tag{3.63}$$

The term, k $(=\pi^2 D/r_o^2)$, is the rate constant, n is the summation integer, D is the diffusion coefficient B in A and r_0 is the radius of particles A. The correlation of this model for polydisperse systems was given by Miyogi[69] (for Jander's model), Sasaki[70] (for Carter and Valensi's model) and Gallagher[71] (for Dünnwald and Wagner's model). The homogeneous model is suitable for porous spheres (pelletized catalysts). The relationships between the continuous and the unreacted-core-shrinking models can be given by the effectiveness factor (see section 3.6.1).

(*b*) *Phase-boundary controlled reactions.* When diffusion through the product layer is so rapid that the reactants cannot combine fast enough at the reaction interface to establish equilibrium, the process becomes phase-boundary controlled. Assuming that the nucleation step occurs virtually instantaneously and that the reaction rate is proportional to the surface area of the fraction of unreacted material

$$\frac{d\alpha}{dt} = \frac{kS_t}{V_0} \tag{3.64}$$

where S_t is the instantaneous surface area of yet unreacted core of particle and V_0 is the original volume of the particle. After various mathematical operations, the equation, analogous to the classical rate equation for gases, is obtained in the form of

$$1-(1-\alpha)^n = \frac{k}{r_0}t \tag{3.65}$$

where n is equal to 1/3, 1/2 and 1 for three-, two- and one-dimensional symmetries, respectively[54]*.

*Note that overall rate constants for topochemical kinetics are inversely proportional to the radius r_0 whereas diffusion kinetics are inversely proportional to the square of the radius.

3.4.4. *Sintering and related phenomena*

A system of solid particles treated under a suitable high temperature undergoes a spontaneous process of hardening where both the surface area and the free energy decreases. The kinetic description of this sintering process is based on the idea that the rate-determining step is the mass flux from the places of the positive to the places of the negative surface curvatures. Frenkel[72] gave the explanation for the sintering of viscous material with Newton's characteristics and later Mackenzie and Shuttleworth[73] for materials with Bingham's body characteristics. Some discrepancies between the theory and the experiment led to the establishment of models where the rate-controlling process is the diffusion of vacancies from the places of negative surface curvatures into the centers of particles (Kingery and Berg[74], etc.).

In general, the sintering process plays a most important part in the formation of ceramic bodies and in powder metallurgy. Hence, it is desirable to list the individual rate-limiting processes to aid in understanding of the overall sintering kinetics. The rate at which the neck volume changes seems to be the best indication for the rate of sintering and is determined by the rate at which atoms move into the neck region. Equating this mass transport flux to the geometric requirement governing the sphere densification gives a series of relationships between neck radius, r, and time t, $r = \text{constant}\ t^m$; where the time exponent m, is characteristic for the particular type of mass transport (see Table 3.8). Because the observation of neck growth is experimentally difficult, it is convenient to determine the linear shrinkage, $\Delta L/L_0$, which is equal to the fractional change in center-to-center particle distance and which exhibits the characteristic time exponent[114] (Table 3.8).

TABLE 3.8

CHARACTERISTIC EXPONENT m IN SINTERING RELATIONS (INITIAL STAGES)

Sintering mechanism	*Neck radius growth* $r = k' t^m$	*Linear shrinkage* $\frac{\Delta L}{L_0}\ \Delta L_{max} = \alpha = kt^m$	*Differential expression* $\frac{d\alpha}{dt} = k\alpha^m$
Evaporation from a convex pore surface and condensation on the concave neck surface.	1/3	no contraction	no contraction
Surface diffusion between the same regions on the solid–vapour surface.	1/7		
Viscous or plastic flow of a solid.	1/2	1	0
Grain boundary diffusion controlled by vacancy formation.	1/4	1/2	−1
Grain boundary diffusion controlled by vacancy movement (both between the same regions along the interparticle boundary).	1/6	1/3	−2
Volume diffusion from the region of interparticle contact into the neck.	1/5	2/2	−2/3

The rate of contraction for a specimen of length L_0, which is composed of monodisperse crystalline spheres of radius a, is given, according to Johnson and Berrin[75], as

$$\left(\frac{\Delta L}{L_0}\right)^{1.03} \frac{\mathrm{d}\left(\frac{\Delta L}{L_0}\right)}{\mathrm{d}t} = \frac{2.63\gamma D_v}{kTa^3} \tag{3.66}$$

for the volume diffusion. If the diffusion takes place along the particle faces, then

$$\left(\frac{\Delta L}{L_0}\right)^{2.06} \frac{\mathrm{d}\left(\frac{\Delta L}{L_0}\right)}{\mathrm{d}t} = \frac{0.7\gamma\Omega b D_B}{kTa^4} \tag{3.67}$$

where $\Delta L\ (= L_0 - L)$ is the linear contraction, γ is the surface energy, Ω is the volume of vacancy, b is the effective gap between two particle faces, D_v and D_B are the bulk and surface diffusion coefficients, respectively, and k is Boltzmann's constant. These equations hold for the initial stages of sintering which involves a significant change in

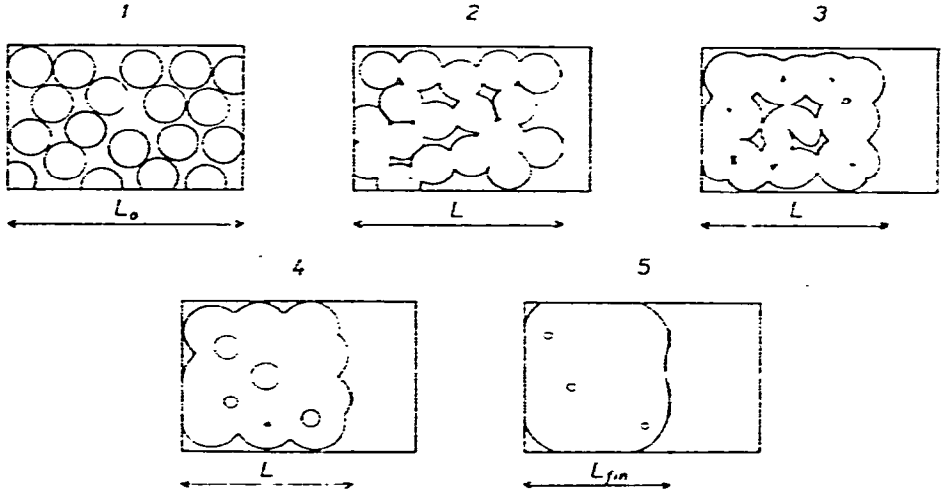

Fig. 3.15. The course of shrinking of powder compact during sintering process.

shape as the necks grow between particles but yield a modest total shrinkage of about ten per cent. The process of sintering involves, however, progressive steps, as shown in Fig. 3.15. The initial stage terminates when grain growth can occur. During the intermediate stage of sintering, where the solid structure formed has a completely continuous pore phase (model 2), grain growth advances and the cross-sectional area of the pore channel decreases. A diffusional equation was selected to calculate the flux of vacancies from the pore channel situated on the edges to the center of the faces of the polyhedron, or

$$\frac{\mathrm{d}P}{\mathrm{d}t} = \frac{-B_t D_v \gamma \Omega}{kT} \tag{3.68}$$

where P is the volume fraction porosity and B_t is a constant related to edge length and possibly to the time dependence of grain size, which may serve to correlate the experimentally obtained curvature in the plots of density vs. time. At about 95 percent of the theoretical density the pores become discontinuous (model 4), thus terminating the intermediate stage. In the final stage where the pores are nearly spherical in shape, they can shrink without changing shape (model 5). The systems, including melts, in the advanced stages of sintering, which sinter by a different mechanism are described by Berežnoj[76] and Kingery[77].

After sintering, the resulting nonporous material is composed of close-packed grains. If the initial particle system is polydisperse, the final grains have a polydisperse character. The larger particles have the center of face curvature inside the grain and they tend to grow at the expense of the smaller grains which have the curvature center outside the particle (model H, Fig. 3.8). The rate of growth is usually diffusion-controlled, as given by the differential equation[78]

$$\frac{dR}{dt} = k\frac{1}{R} \tag{3.69}$$

where R is the radius (size) of the particle.

A similar phenomenon is the spontaneous coarsening of precipitants. In a polydisperse system the number of mean-sized particles grows because certain particles disappear, feeding, in fact, on the growth of larger particles. This process is associated with the decrease of interfacial free energy. After some simplifications, Greenwood[79] deduced the following equation

$$R\left(\frac{dR}{dt}\right) = \frac{2D_v V_m \gamma}{RT}\frac{C}{C^*}\left(\frac{1}{R_m} - \frac{1}{R}\right) \tag{3.70}$$

where C and C^* are the concentrations in a saturated solution in equilibrium with the planar interface and with the precipitant particles of radius R, respectively; V_m is the molar volume of the precipitant, R_m is the average particle size and γ is the interfacial energy.

The theoretical models for sintering are difficult to reformulate in terms of surface area. Although the ratio of surface to volume of a particle depends to a certain extent on its shape, it varies inversely with the diameter of particle. The total free energy of a large number of fine particles is therefore greater than that of a smaller number of large particles or even a solid block of equal volume. It is thus reasonable to assume that the driving force for fine-powder sintering is the reduction of total surface area and total free energy. As the surface energy is proportional to the surface area, A, it can be written[80,81] similarly to the above-introduced time exponent

$$dA/dt = -k_s A t^{-n} \text{ and/or } dA/dt = -k_s'(A - A_f)^{-n'} \tag{3.71}$$

where k_s is the temperature dependent constant and A_f is the surface area after the sintering is completed.

3.5. Molecular description of heterogeneous processes

3.5.1. Role of defects in solid-state processes

The explanation of reactions in liquids and gases is not difficult because the reactant mixtures occur on the molecular level. The existence of uniform concentration at the reaction zone is thus acceptable. In solid-state reactions the concepts based on concentration are of little significance and the kinetics should be expressed in terms of both spatial and time coordinates, as shown in section 3.4. But such kinetic equations derived from the overall reaction velocities are insufficient to characterize in detail the intrinsic mechanism because many plausible kinetic paths, although differing in details, lead often to the same kinetic law. Thus for a better understanding of solid-state reactions it is desirable to establish still another model on the atomic level of elementary processes in the solid network[85–99]. This model is based on the knowledge of the nature and properties of lattice imperfections. Such defects must either be created or destroyed, move, interact, aggregate and/or become ordered to make possible a solid-state reaction. From this point of view the surface represents, in fact, one of the most important imperfections of the solid-state lattice. At a temperature above absolute zero a finite crystal may present some of the following defects:

1) *Point defects*: *a*) Atomic (vacancies, interstitial atoms or ions, foreign atoms or ions in the proper lattice sites and/or in interstitial spots); *b*) Electrical (free electrons or holes); *c*) Thermal (phonons).

2) *Line defects* dislocations.

3) *Plane defects* stacking fault, steps, discontinuity at atomically flat surface.

4) *Volume defects* inhomogeneities, lattice distortions.

All solid-state reactions undergo one of the following steps during their transition states:

1) The creation of a defect.

2) The association of defects into small clusters (prenucleus formation) which, although distorted, is still part of the host lattice.

3) The transformation of a prenucleus into a definite product domain (nucleus formation).

4) The transport of matter through the solid by some type of a defect diffusion process.

5) Growth of nuclei by accretion of defects.

6) In some cases also the formation of a gas molecule and its desorption

The existence of defects gives the atoms an opportunity to move across the solid lattice as a necessary condition for any solid-state process. It is plausible to presume that in an ideal lattice (perfect solid) no reaction could occur.

3.5.2. Creation of defects

The sources of point defects are often processes taking place at the phase boundary. For example, in a perfect crystal of NiO in contact with an atmosphere of a given partial pressure of oxygen, the equilibrium concentration of defects is established spontaneously. This process starts on the crystal surface where electronegative gaseous oxygen is absorbed as the O^{2-} ion, thus drawing away two electrons from two neighboring Ni^{2+} ions. The two holes created (Ni^{3+}) are likely to move into the crystal bulk while Ni^{2+} underneath climb up to the surface to lengthen the boundary lattice along with new O^{2-} ions. The difference in the concentration of holes and vacancies is balanced by the diffusion flux if the crystal is put in good contact with metallic nickel. This in fact simulates the actual conditions during the surface oxidation of nickel, which is the simplest case of a diffusion-controlled process leading to the parabolic kinetic law, as discussed in section 3.3.4 (the defect concentration on the NiO/Ni interface would be different than that on the NiO/O_2 surface creating a permanent concentration gradient across the NiO layer which serves as a driving force for the diffusion process resulting in the gradual build-up of the NiO layer[88]).

A number of studies of sintering in oxides were concerned with the effect of impurities on sintering rate. Since this rate depends upon the diffusion coefficient, all factors which change the vacancy concentration will also change the sintering rate. Thus, the addition of Li_2O to ZnO was found to increase the sintering rate, evidently because it adds oxygen vacancies and the slow step is expected to be the diffusion of anions.

Another source of defects may be the curvature of the phase-boundary, as discussed in section 3.4.4. A surface with a negative curvature contains an excess of vacancies in comparison to the crystal bulk[89]. The highest concentration of vacancies is therefore in the regions where the surfaces are most sharply curved and the free energy change is most favorable for vacancy generation on the points of two particle contacts. This accounts for the preferential growth of the joining necks[89,90] by vacancy movement at grain boundaries. It gives a net flow of atoms in the reverse direction and leads to consequent shrinkage and final densification. The function of the grain boundary as a sink for vacancies is a key concept. It was proven experimentally in the case of pores isolated from grain boundaries which do not shrink, i.e., no concentration gradient appears to permit diffusion. The second most important phenomenon in solid-state reactions is diffusion. In addition, it should be mentioned that the generation and diffusion of defects can be facilitated by stress, magnetic fields, etc.

3.5.3. Elementary mechanism of diffusion

The only passage for mass transport in a perfect lattice of a cubic close-packed structure interpenetrates the array of tetrahedral or octahedral interstices. Any discontinuity, such as a dislocation line, enables the diffusion to proceed with more ease than through a perfect lattice. In general, the transport of matter in solids is

accomplished through the point-defects-walk process and depends upon the concentration and the mobility of defects. Both these parameters depend on the crystal structure and large number of published articles have appeared on this[91].

In principle, when two solid crystals are in contact (see Figs. 3.13 and 3.14), the diffusion of components A and B takes place at the same time across the interface AB. The initial position of this interface (which may be indicated by an inert material) will not change if the rate of diffusion of both components is of the same value. If the mass, charge and size of the diffusing particles of each component are different, their mobility differs also. The amount of the more diffusive component transported per unit time across the original interface is larger and the actual interface shifts, as first reported by Hartley[92], and Smigelshas and Kirkendal[93].

Diffusion may also be affected by the presence of paths formed by any system of defects, dislocations, stacking faults, grain boundaries, etc. In ionic crystals, the transport of matter may also arise because of a different mobility of atomic and electronic defects, due to the influence of an externally applied electric field. In some cases, the difference between the diffusion rate of both components is considerable. In extreme cases, where the transport of one component is high due to the presence of highly mobile vacancies, deformation of a solid body can occur, as illustrated in Fig. 3.16. This is caused by creation of pores in the places to which the vacancies are delivered[94,95].

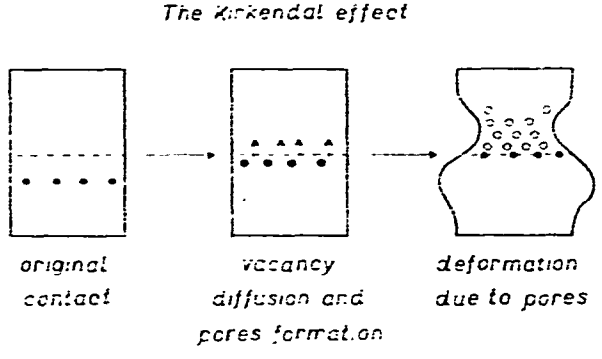

Fig. 3.16. Deformation of two reacting solids due to the different mobilities of diffusing species (the dots mark the line of contact).

3.5.4. Prenucleus formation

The formation of a product phase in a solid-state reaction implies that, at some stages, entities foreign to the perfect host reactant solid, namely, vacancies, interstices, foreign atoms or ions, or a simple combination of point defects, must aggregate into an ordered array, which ultimately becomes a crystal of the product phase. Even though there is no direct evidence for this process, it is clear that the existence of attractive interactions between defects is a necessary condition for aggregation and phase separation[96]. Point defects, whether interstitial, substitutional or vacancy, will

tend to display repulsive interactions because of elastic and coulombic interactions. However, charged simple defects tend to associate with simple defects of opposite charge, for instance,

(a) Electrons with vacant anion sites (to form F-centres $e/\square^{-}$).

(b) Anion vacancies with anions of greater charge.

(c) Migration of point defects to dislocations to relieve elastic stresses, etc.

The simple case of an aggregation of F-centres in sodium chloride is demonstrated in Fig. 3.17 where the prenucleus, marked by a dashed line, is the precursor of a new phase to form Na metal as it becomes large enough to be thermodynamically stable.

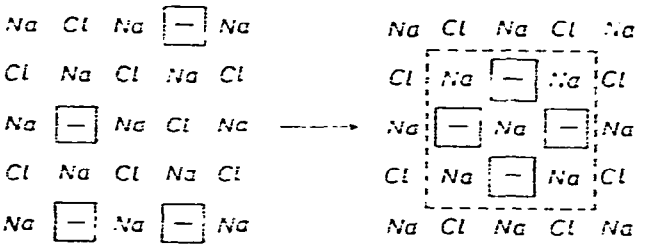

Fig. 3.17. Prenucleus formation by ordering of defects.

The nuclei growth is often conditioned by the existence of screw dislocations which make possible a rapid incorporation at relatively low concentrations. The screw dislocations are formed in small prenuclei at the surface of a matrix crystal by a mechanism where the coherency stress is relieved by the generation of dislocations which intersect the surface and promote the spiral growth[97]. This model also fits experimental observations for epitaxial growth of reaction products on a reactant single crystal, where the crystals of product hold certain phase (epitaxe) or volume (topotaxe) orientation with regard to the host structure. The direction of the screw dislocation is given by the slip in the product network. If the single crystal surface is appropriate, then the screw dislocation will emerge from the free surface and a crystal of the product will grow with preservation of the built-in epitaxial relationship.

If a gaseous product is created by a solid-state reaction, the nucleation mechanism on the energetically rich points is also to be dealt with. One of the investigated processes is the thermal decomposition of azides[96]. It was shown that the first step was the absorption of radiation, as a result of which an electron is excited from the valence band (N_3 band) thus producing a positive hole in the N_3 band and an electron in the conduction band (M^{+} band). The conduction electron is subsequently trapped to produce the free metal product (M) and the positive hole associates with a suitable site to give rise to the gaseous product.

It is quite evident that there are additional aspects such as the influence of

structure, the conditions of experiment, material history, on solid-state reactions which have not been included in this review.

3.5.5. Interpretation of kinetic equations

A knowledge of the mechanism of the process enables the interpretation of the rate equation in terms of molecular quantities characterising the system studied. An excellent example of such an approach is the Wagner theory of copper tarnishing[84-87]. The reaction in the steady state proceeds in three successive stages:

1) An oxygen molecule striking the surface of Cu_2O dissociates and is chemisorbed in a monolayer which creates Cu^+ vacancies and Cu^{2+} holes.

2) The vacancies and holes diffuse through the Cu_2O layer to the Cu_2O–Cu interface.

3) Atoms jump into the vacancies and free electrons fill the holes.

Diffusion is the slowest process in the reaction and is the rate determining step. Using this idea, Wagner has derived an equation for the rate of growth of an oxide layer,

$$\frac{x}{V_c}\frac{dx}{dt} = \frac{300}{Fz_{Cu} + e_0 N}\int_{\mu_{O_2}(0)}^{\mu_{O_2}(x)} \sigma t_e (t_{Cu^+} + t_{O^-})\, d\mu_{O_2} \tag{3.72}$$

where x = the oxide layer thickness
V_c = the volume of Cu_2O per Cu atom
F = Faraday (96 500 coulombs)
N = Avogadro's number
e_0 = elementary charge
$|z_{Cu^+}|$ = charge of Cu^+ ions
σ = specific conductance of Cu_2O layer
t_i = transfer numbers
μ_{O_2} = chemical potential of O^{2-} ions, the value of which on Cu/Cu_2O boundary is $\mu_{O_2}(0)$ and equals $\mu_{O_2}(x)$ on the Cu_2O/O_2 boundary.

For our case, t_e for holes is unity, t_i for oxygen equals zero, O^{2-} does not move and t_i for Cu^+ vacancies could be measured by an electrochemical technique.

Electrical conductivity of Cu_2O depends on the concentration of holes, which is a function of the partial pressure of oxygen

$$\sigma = \sigma^0 \times p_{O_2}^{1/7} \tag{3.73}$$

where σ^0 is the conductivity at $p_{O_2} = 1$ atm. Introducing

$$d\mu_{O_2} = RT\, d \ln p_{O_2} \tag{3.74}$$

and using eqn. (3.73), one obtains by integration of eqn. (3.72)

$$\frac{x}{V_c}\frac{dx}{dt} = \frac{300\sigma^0 t_{Cu^+} RT}{2FNe_0}([p_{O_2}(x)]^{1/7} - [p_{O_2}(0)]^{1/7}) \tag{3.75}$$

The rate of oxidation must be a linear function of $(P_{O_2})^{1/7}$. All constants on the

right-hand side of eqn. (3.75) can be measured directly. The calculated rate of oxidation is in good agreement with the value obtained from the kinetics measurement. The results represent excellent proof of the suggested mechanism of the process.

From the above it can be seen that the field of heterogeneous reactions is vast*. and is difficult to classify and describe in an objective manner. It is the object of this review to satisfy the present need of a more critical and detailed approach to the physicochemical studies of heterogeneous reactions with regard to the methods of thermal analysis. Bearing in mind the broader aspects of thermal analysis, it is useful to include a typical technological appraisal of the above problems.

3.6. Heterogeneous processes under actual experimental conditions

3.6.1. Engineering approach

In the preceding part more-or-less idealized conditions were considered to analyze the physico-chemical character of the processes investigated. It is possible to separate experimentally the individual processes as referred to the above-suggested models. On the other hand, the engineering approach to the description of a heterogeneous reaction based on the shrinking unreacted-core model of a system of single solid particles, is formulated from a procedural, macroscopic point of view[100–107]. The effects accompanying diffusional and hydrodynamic conditions are superimposed on the main physico-chemical process of the new phase formation. Furthermore, the engineers have a more realistic standpoint to the conditions under which the reaction actually proceeds*.

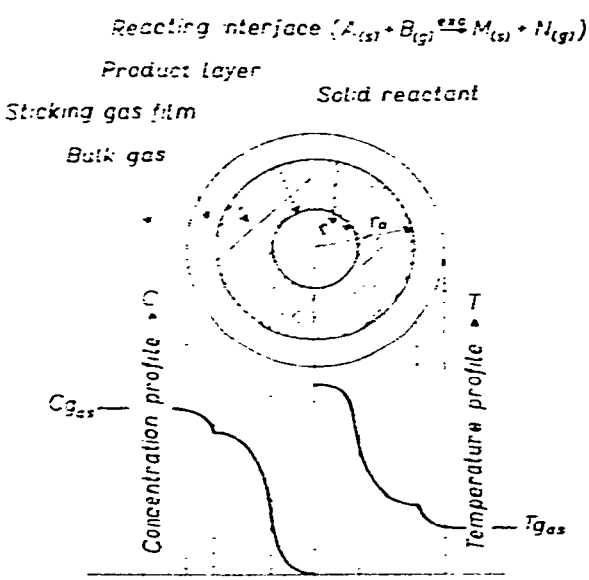

Fig. 3.18. Actual temperature and concentration profiles for a shrinking-core model of an exothermic reaction.

*See *Note added in proof* on p. 443.

In Fig. 3.18, the actual profile[102] of temperature and concentration for a shrinking-core model of an exothermic reaction is shown in order to aid in understanding the actual conditions during a heterogeneous process (compare with Fig. 3.5). In the design of heterogeneous chemical reactors, the following five rate-determining steps are basically accounted for (not considering heat transfer): (1) diffusion of a gaseous reactant across the gaseous film into the solid particle surface; (2) penetration of the gaseous reactant through the layer of inert product into the reacting interface; (3) chemical-like reaction at the interface; (4) diffusion of the gaseous product back to the surface; and finally (5) diffusion of the gaseous product through the adhering gaseous layer. Steps (1) and (4) and/or (2) and (5) are mathematically almost identical differing only in the sign. In the usual engineering terms, the rate-determining step can be found by means of a plot[4] of the normalized time ratio, t/τ, vs. the ratio of reacting r per initial particle radius r_0. The term, t, is the instantaneous time and τ is the time necessary for total process completion (see Fig. 3.19). In addition, it is necessary to take into account not only the mass but also

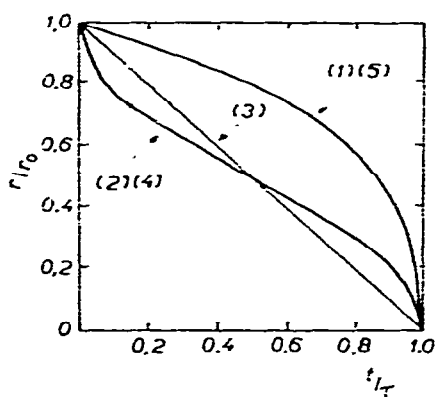

Fig. 3.19. The determination of five possible rate-limiting steps.

the heat balance which results in a complicated relation, particularly for exothermal reactions. The best approach seems to be to analyze the effects of the heat of reaction, mass and heat transfer, etc., on the overall reaction rate of a single particle in the conventional terms of the effectiveness factor, η_s, defined as:

η_s = *actual (overall) reaction rate* (reaction rate obtainable when the reaction site is exposed to the gas concentration and temperature of the bulk gas phase).

This effectiveness factor, η_s, is based on the concentration and temperature in the bulk gaseous phase, which remains constant during the reaction and corresponds to the dimensionless rate per unit surface of reaction interface. When η_s is plotted against the fractional conversion, α, of the solid reactant, the thermal instabilities and the transitions in the rate-controlling phases, provided they exist, are easily pointed out, as shown by Ishida and Wen[100]. Furthermore, a positive slope of the α vs. η_s curve ($d\eta_s/d\alpha > 0$) indicates the existence of a geometrical instability in which the

reaction interface may become uneven and the shrinking-core model may not be applicable.

3.6.2. Thermal conditions during heterogeneous processes

The processes considered in the preceding sections can proceed under various conditions given by both the time and space distribution of temperature throughout the system investigated. In principle, the following four cases may be distinguished:

(1) The temperature is constant in time and uniform throughout the system.

(2) The temperature is time dependent (e.g., linearly or inversely proportional to time) but is independent upon space coordinates in the system.

(3) The temperature is not dependent upon time but is a function of the space coordinates in the system.

(4) The temperature varies with either time or the location in space coordinates.

The first two cases are convenient for ordinary kinetic studies, as the process can be realized by a defined path. It is, of course, to be taken into account that there arises an inevitable difference between the desired and actual experimental conditions[115]. Actually, the first approach is the groundwork of "classical" isothermal techniques of investigation while the second, which is not widely accepted as yet, will next be considered in detail[102,103].

In connection with the last two points, it seems necessary to stress the thermal instability of some exothermic heterogeneous reactions studied under non-isothermic conditions. As an example, the combustion of solid and/or liquid fuels and some special types of the reduction by hydrogen (FeS) or the oxidation by oxygen (ZnS)

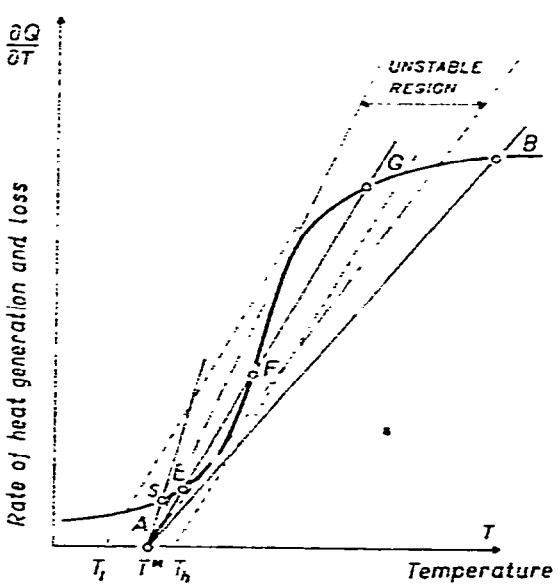

Fig. 3.20. Schematic diagram of rate of heat generation against temperature (see text).

may serve. This thermal instability was first pointed out by Van Heerden[104] while studying different types of solid–gas reactions and later analyzed by Cannon and Denbigh[105]. In the case of the oxidation of ZnS, two main points should be noted:

(1) The way in which the curves of heat generation and heat loss intersect each other.

(2) The variation of the impedance of the reaction product build up against heat loss passage.

A schematic diagram of the first case, as illustrated in Fig. 3.20, shows the sigmoidal shaped curve of heat generation and the lines of heat loss for an exothermic solid–gas reaction as a function of temperature. At lower temperatures, the heat generation is controlled by the reaction kinetics and the temperature dependence is exponential. However, at higher temperatures the diffusion through the product layer becomes the rate-controlling process and the rate of heat generation is almost temperature independent. If the rate of heat-loss is rapid, the line of heat loss intersects the heat generation curve in the region of comparatively low temperatures (point S) and a stationary state is established where the rate determining process is the phase-boundary reaction. Similarly, at very low rates of heat loss (point B) the stationary state is also attained with the diffusion as the rate-determining step. Within the region between points E and G, thermal instability is then created (see dashed lines). Although at point F heat loss is equal to heat generation, it is a metastable point in the sense that any small decrease of temperature at the reaction surface will cause the system to fall to point E and any small increase will cause the system to rise to point G. Both changes are accompanied by a sudden change in the rate determining process. It can also be seen that only one crossing point exists when the temperature of the surrounding gas, T^*, is either extremely low (T_c) or extremely high (T_h) (see dotted lines parallel to $\overline{EFG}$). Criteria of this instability are given by Aris[106] and Wen and Wang[107].

The second cause of instability can be the growth of the product layer[100]. A small deviation in the layer thickness tends to expand, resulting finally in an autocatalytic type of the layer build up. With the shrinking core of particles, the generation of heat is decreased, but, at the same time, the rate of heat loss is also decreased due to the increasing thickness of product layer. If the second phenomenon overcomes the first one, the interface temperature is elevated up to the point where the system becomes unstable.

Note added in proof

For comparison see also the classification made from the viewpoint of metallography: spinodal and eutectoid decompositions, precipitation from solid solutions, ordering reactions, martensitic, bainitic and massive transformations (C. W. Wayman, *Ann. Rev. Mater. Sci.*, 1 (1971) 185) and/or the approach which considers the equilibrium background in solid-state kinetics: invariant, variant and permanent

processes starting from a stable or metastable initial state, processes characterized by multiple parameters and combined processes (P. Holba and J. Šesták. *Proc. 6th Czech. Conf. Therm. Anal., October 1973*, SVŠT, Bratislava, 1973, pp. P1–P12).

REFERENCES

1 B. Delmon, *Introduction à la cinétique hétérogène* (Publ. de l'Institut français du pétrole), Édition Technique, Paris, 1969.
2 D. A. Young, *Decomposition of Solids*, Pergamon Press, Oxford, 1966.
3 W. E. Garner, (editor), *Chemistry of the Solid State*, Butterworths, London, 1955.
4 O. Levenspiel, *Introduction to the Design of Chemical Reactors*, Wiley, New York, 1962.
5 S. L. Friess, E. S. Lewis and A. Weissberger (editors), *Investigation of Rates and Mechanisms of Reactions*, Interscience, New York, 1961.
6 G. Boldyrev, *Methods of Investigations of Thermal Decomposition of Solids State*, Tomsk, USSR, 1958.
7 S. Glasstone, K. Y. Laidler and H. Eyring, *The Theory of Rate Processes*, McGraw-Hill, New York, 1941.
8 M. Polanyi and E. Wigner, *Z. Phys. Chem.*, A139 (1928) 439.
9 R. D. Shannon, *Trans. Faraday Soc.*, 60 (1964) 1902. (See also I. Proks, *Chem. Zvesti*, 20 (1966) 697).
10 H. F. Cordes, *J. Phys. Chem.*, 72 (1968) 2185.
11 C. Zener, *Imperfections in Nearly Perfect Crystals*, Wiley, New York, 1952, Chap. II.
12 I. G. Murculescu and E. I. Segal, *Rev. Roum. Chim.*, 10 (1966) 307.
13 M. G. Evans and M. Polanyi, *Trans. Faraday Soc.*, 34 (1938) 11.
14 C. E. Birchenall, *The Mechanism of Diffusion in Solids, in Reactivity of Solids*, Elsevier, Amsterdam, 1960.
15 M. B. Pahart and R. Basu, *J. Chim. Phys.*, 68 (1971) 753.
16 L. Madelkern, *Crystallization of Polymers*, McGraw–Hill, New York, 1964.
17 G. M. Pen'enkov and B. P. Lebedëv, *Chemical Kinetics and Catalysis*, Izd. Moskovskogo Univ., Moscow, 1961.
18 S. W. Benson, *Thermochemical Kinetics*, Wiley, New York, 1968.
19 D. M. Himmelblan, C. R. Jones and K. B. Bischoff, *Ind. Eng. Chem.*, 6 (1967) 539.
20 R. W. Brandshaw and B. Davidson, *Chem. Eng. Sci.*, 24 (1969) 1519.
21 S. D. Foss, *Chem. Eng. Sci.*, 26 (1971) 485.
22 I. G. Gay, *J. Phys. Chem.*, 75 (1971) 1610.
23 Y. P. Tang, *Ind. Eng. Chem.*, 10 (1971) 321.
24 W. H. Sachs, *Acta Chem. Scand.*, 25 (1971) 762.
25 J. Lee, *Int. J. Chem. Kinetics*, 3 (1971) 491.
26 M. M. Pavluchenko and A. S. Meteiski, *Dokl. Akad. Nauk SSSR*, 25 (1971) 607.
27 E. A. Dorko and R. W. Crossley, *J. Phys. Chem.*, 76 (1972) 2253.
28 D. W. Kingery (editor), *Kinetics of High Temperature Processes*, Wiley, New York, 1959.
29 J. C. Jungers and J. C. Balaceanu, *Heterogeneous Reactions and Catalysis in Investigations of Rates and Mechanisms of Reactions*, in S. L. Friess, E. S. Lewis and A. Weisseberger (editors), *Investigation of Rates and Mechanisms of Reactions*, Interscience, New York, 1961.
30 P. P. Budnikov and A. M. Ginstling, *Reaction in Mixtures of Solids*, Promstroizdat, Moskva, 1961.
31 J. W. Christiansen, in R. W. Cahn (editor), *Physical Metallurgy*, North-Holland Publ. Co., Amsterdam, 1965.
32 E. Rutner, P. Goldfinger and J. P. Hist (editors), *Condensation and Evaporation of Solids*, Gordon & Breach, New York, 1964.
33 J. L. Margrave (editor), *The Characterisation of High Temperature Vapors*, Wiley, New York, 1967.
34 J. Crank, *Mathematics of Diffusion*, Clarendon Press, Oxford, 1956.
35 R. B. Bird, W. E. Stewart and E. N. Lightfoot, *Transport Phenomena*, Wiley, New York, 1965.
36 A. W. Hixson and J. H. Crowell, *Ind. Eng. Chem.*, 23 (1931) 923, 1002 and 1160.
37 J. Hlaváč, *Silikáty*, 7 (1963) 242.

38 D. W. Readey and A. R. Cooper, *Chem. Eng. Sci.*, 21 (1966) 917.
39 S. C. Stavrinon and A. A. Blumberg, *J. Phys. Chem.*, 64 (1960) 1438.
40 M. Volmer and A. Weber, *Z. Phys. Chem. (Leipzig)*, 119 (1925) 277.
41 R. Becker and W. Döring, *Amer. J. Phys.*, 24 (1935) 719.
42 R. Becker, *Amer. J. Phys.*, 32 (1938) 128.
43 G. Borelius, *Amer. J. Phys.*, 28 (1938) 567 and *Trans. AIME*, 191 (1951) 477.
44 G. Hobstetter, *Trans. AIME*, 180 (1949) 121.
45 W. J. Cahn and J. E. Hilliard, *J. Chem. Phys.*, 28 (1958) 258; 31 (1959) 688.
46 D. R. Uhlmann and B. Chahmers, *Ind. Eng. Chem.*, 57 (1965) 19.
47 J. Burke, *Phase Transformation in Metals*, Pergamon Press, London, 1965.
48 P. W. M. Jacobs and F. C. Tompkins, in W. E. Garner (editor), *Chemistry of the Solid State*, Butterworths, London, 1955, p. 184.
49 K. L. Mampel, *Z. Phys. Chem.*, A 187 (1940) 235.
50 B. V. Yerofeyev, *Dokl. Akad. Nauk SSSR*, 52 (1946) 511.
51 A. N. Koglomorov, *Izv. Akad. Nauk USSR*, (1937) 355.
52 W. A. Johanson and R. F. Mehl, *Trans. AIME*, 135 (1939) 416.
53 M. Avrami, *J. Chem. Phys.*, 7 (1939) 1103; 8 (1940) 212 and 9 (1941) 177.
54 S. F. Hulbert, *J. Brit. Ceram. Soc.*, (1970) 11.
55 J. Šesták, *Phys. Chem. Glasses*, December 1973, in press.
56 E. G. Prout and F. C. Tompkins, *Trans. Faraday Soc.*, 40 (1944) 488; 42 (1946) 468.
57 H. Schulze, *Glas*, Vieweg & Sohn, Braunschweig, 1965.
58 B. Chalmers, *Principles of Solidification*, Wiley, New York, 1964.
59 C. Kroger and G. Ziegler, *Glastech. Ber.*, 26 (1953) 346; 27 (1954) 199.
60 A. E. Nielsen, *Kinetics of Precipitation*, Pergamon Press, Oxford, 1964.
61 C. Zener and C. Wert, *J. Appl. Phys.*, 21 (1950) 5.
62 F. S. Ham, *J. Appl. Phys.*, 30 (1959) 1518.
63 R. F. Strickland-Constable, *Kinetics and Mechanism of Crystallization*, Academic Press, New York, 1968.
64 E. R. Carter, *J. Chem. Phys.*, 34 (1961) 2010; 35 (1961) 1137.
65 G. Valensi, *C.R. Acad. Sci.*, 202 (1936) 309.
66 W. Komatsu and T. Uemura, *Z. Phys. Chem. (Frankfurt am Main)*, 72 (1970) 59.
67 H. Dünwald and C. Wagner, *Z. Phys. Chem. B*, 24 (1934) 53.
68 B. Serrin and R. T. Erlickson, *J. Chem. Phys.*, 9 (1941) 742.
69 B. Miyogi, *J. Jap. Ceram. Soc.*, 59 (1951) 132.
70 B. Sasaki, *J. Amer. Ceram. Soc.*, 47 (1961) 512.
71 K. J. Gallagher, in G. M. Schwab (editor), *Reactivity of Solids*, Elsevier, 1965, p. 195.
72 J. Frenkel, *Zh. Fiz. Khim.*, 9 (1943) 385.
73 J. K. MacKenzie and R. Shuttleworth, *Proc. Phys. Soc. (London)*, B 62 (1949) 833.
74 W. D. Kingery and M. Berg, *J. Appl. Phys.*, 26 (1955) 1206.
75 D. L. Johnson and L. Berrin, in G. C. Kuczyński, N. A. Hooton and C. F. Gibbon (editors), *Sintering and Related Phenomena*, Gordon & Breach, New York, 1967.
76 J. E. Berežnoj, *Fizika Spekania*, Izd. Nauka, Moskva, 1967.
77 W. D. Kingery, *J. Appl. Phys.*, 30 (1959) 301.
78 J. E. Burke and D. Turnbull, *Progr. Metal Phys.*, 3 (1952) 220.
79 G. W. Greenwood, *Acta Met.*, 4 (1956) 243.
80 S. Y. Gregg, R. K. Racker and K. H. Wheatley, *J. Chem. Soc.*, (1955) 45.
81 D. Nicholson, *Trans. Faraday Soc.*, 61 (1965) 990.
82 M. M. Pavlyuchenko, *Heterogeneous Chemical Reactions*, Nauka i těchnika, Minsk, 1964.
83 M. M. Pavlyuchenko, *Zh. Fiz. Khim.*, 29 (1955) 39.
84 V. Šatava, *Silikáty*, 4 (1960) 67.
85 F. A. Kröger, *The Chemistry of Imperfect Crystals*, North-Holland Publ. Co., Amsterdam, 1964.
86 K. Houffe, *Reaktionen an und in festen Stoffen*, Springer, Berlin, 1955.
87 H. Schmalzried, *Festkörperreaktionen*, Verlag Chemie, Weinheim, 1971.
88 O. Kubaschewski and O. Von Goldbeck, *Z. Metallk.*, 39 (1948) 158.
89 W. D. Kingery and M. Berg, *J. Appl. Phys.*, 26 (1955) 1205.
90 L. J. Bonis and H. H. Hansner (editors), *Fundamental Phenomena in Material Sciences*, Pergamon Press, New York, 1964.

91 F. C. Tompkins, *Influence of Structure on Solid-State Reactions*, in *The Reactivity of Solids*, Butterworths, London, 1965, p. 387.
92 G. S. Hartley, *Trans. Faraday Soc.*, 42 B (1946) 6.
93 A. D. Smigelskas and E. O. Kirkendall, *Trans. AIME*, 171 (1947) 130.
94 L. S. Darken, *Trans. AIME*, 175 (1948) 184.
95 Th. Herrmann and A. Kottmann, *Z. Metallk.*, 44 (1953) 139.
96 F. P. Bowden and A. D. Yoffe, *Fast Reactions in Solids*, Butterworths, London, 1958.
97 A. L. G. Rees, *Chemistry of the Defect Solid-State*, Methuen, London, 1954.
98 A. L. G. Rees, *Elementary Processes in Solid-State Reactions*, Conference of Electrochemistry, Sydney, 1963 (Proceedings, p. 3).
99 Y. H. Crawford and L. H. Slifkin, *Annual Review of Material Science*, Vol. 1, Annual Reviews Inc., Palo Alto, California, 1971.
100 M. Ishida and C. Y. Wen, *Chem Eng. Sci.*, 23 (1968) 125.
101 S. Yagi and D. Kunii, *Chem. Eng. (Tokyo)*, 19 (1955) 500.
102 R. J. Williams, A. Calveto and R. E. Cunningham, *J. Catal.*, 19 (1970) 363.
103 J. Shen and J. M. Smith, *Ind. Eng. Chem. Fundam.*, 4 (1965) 293.
104 C. Van Heerden, *Ind. Eng. Chem.*, 45 (1953) 1242.
105 K. J. Cannon and K. G. Denbigh, *Chem. Eng. Sci.*, 6 (1957) 155.
106 R. Aris, *Ind. Eng. Chem. Fundam.*, 6 (1967) 315.
107 C. Y. Wen and S. C. Wang, *Ing. Eng. Chem.*, 62 (1970) 30.
108 M. E. Fine, *Phase Transformations in Condensed Systems*, McMillan Co., New York, 1964.
109 J. W. Christian, *The Theory of Transformations in Metals and Alloys*, Pergamon Press, New York, 1965.
110 W. Jander, *Z. Anorg. Allg. Chem.*, 163 (1927) 1.
111 V. F. Zhuravlev, I. G. Lesokhin and R. G. Tempelman, *J. Appl. Chem. USSR*, 21 (1948) 887.
112 R. M. Barrer, *Phil. Mag.*, 35 (1944) 802.
113 A. M. Ginstling and B. I. Brounshtein, *J. Appl. Chem. USSR*, 23 (1950) 1327.
114 J. H. Brophy, R. M. Rose and J. Wulff, *The Structure and Properties of Materials*, Vol. III, *Thermodynamics of Structure*, Wiley, New York, 1967.
115 A. W. D. Hills, *Heat and Mass Transfer in Process Metallurgy*, Elsevier, New York, 1967.